MSc

2.º CICLO

FCUP
ICBAS
2020/
2021

Chemoprevention of Skin Cancer Through Mutant p53 Reactivation

Rita Do Carmo Ribeiro

U.PORTO
FACULDADE DE CIÊNCIAS
UNIVERSIDADE DO PORTO

U.PORTO
ICBAS | INSTITUTO DE CIÊNCIAS BIOMÉDICAS ABEL SALAZAR
SCHOOL OF MEDICINE AND BIOMEDICAL SCIENCES

Chemoprevention of Skin Cancer Through Mutant p53 Reactivation

Rita Do Carmo Ribeiro

Dissertação de Mestrado apresentada à
Faculdade de Ciências da Universidade do Porto e Instituto de Ciências Biomédicas Abel Salazar em
Mestrado em Bioquímica

2021

U.PORTO
FACULDADE DE CIÊNCIAS
UNIVERSIDADE DO PORTO

U.PORTO
ICBAS | INSTITUTO DE CIÊNCIAS BIOMÉDICAS ABEL SALAZAR
SCHOOL OF MEDICINE AND BIOMEDICAL SCIENCES

Chemoprevention of Skin Cancer Through Mutant p53 Reactivation

Rita do Carmo Ribeiro

Mestrado em Bioquímica

Faculdade de Ciências da Universidade do Porto e Instituto de Ciências Biomédicas Abel Salazar

2021

Orientador

Lucília Helena Ataíde Saraiva, Professor Auxiliar, Faculdade de Farmácia da Universidade do Porto

Coorientador

Marco Aurélio Gouveia Alves, Investigador Convidado Equiparado Investigador Auxiliar, Instituto de Ciências Biomédicas Abel Salazar

Todas as correções determinadas

pelo júri, e só essas, foram efetuadas.

O Presidente do Júri,

Porto, _____/_____/_____

All religions, arts and sciences are branches of the same tree. All these aspirations are directed toward ennobling man's life, lifting it from the sphere of mere physical existence and leading the individual towards freedom.

- Albert Einstein

Acknowledgements

I would like to start this thesis by acknowledging and expressing my gratitude to the people who have been crucial in my path. Thank you all for your support professionally and also your friendship and encouragement.

First of all, I want to give my sincere thank you to my supervisor, Professor Lucília Saraiva, for once more receveing me in her brilliant team with open arms. It was a wonderful opportunity to learn from an inteligent and fierce woman with such dedication to science and investigation.

To Dr. Marco Alves, my co-supervisor, thank you for also welcoming in your laboratory and amazing team.

To Dr. Joana Loureiro, the best tutor and partner I could ever ask for. Thank you for making me independent in the lab and giving me the freedom to make mistakes and learn from them. Thank you for guiding me during work hours but also for the advices on my professional journey. Your commitment, hard work and altruism cannot go unoticed.

To all my colleagues, Mariana, Juliana, Joana, Liliana, Helena and João, thank you so much for your companionship and guidance.

À minha família, pelo amor e pelas gargalhadas de domingo. Em particular à minha mãe, por me apoiar em tudo e respeitar as minhas decisões e por todos os ensinamentos valiosos.

A special thank you to my life partner, Pedro. Thank you for all the love and the laughs, and also for the support and patience. Everything in life is wonderful by your side.

To my friends, for the friendship and support that enabled us to keep in touch for so many years. Specially to my lovely friend and colleague Eduarda, for accompanying me in these 5 years in university.

Funding

This work received financial support from PT national funds (FCT/MCTES, Fundação para a Ciência e Tecnologia and Ministério da Ciência, Tecnologia e Ensino Superior) through grant UID/QUI/50006/2019; M.G. Alves (IFCT2015 and PTDC/MEC-AND/28691/2017) and UMIB (UIDB/00215/2020 and UIDP/00215/2020).

Resumo

O cancro da pele (CP), incluindo o melanoma maligno e o CP não-melanoma, está entre os tipos de cancro mais incidentes. A radiação ultravioleta (UVR) constitui um dos principais fatores de risco associados ao CP. Os seus principais efeitos biológicos na pele incluem a indução de danos no DNA, nomeadamente a formação de dímeros de pirimidina ciclobutano e pirimidina (6-4) pirimidona fotoprodutos, a produção de espécies reativas de oxigénio (ROS), e a inflamação. Os danos no DNA induzidos pela radiação UV promovem a mutagénese de proto-oncogenes e supressores tumorais importantes, tal como a proteína p53. De facto, mutações no gene *TP53* surgem em fases precoces da carcinogénese da pele e têm um papel crucial na transformação maligna. O aumento da incidência de CP indica que as estratégias de prevenção contra o CP, incluindo o uso de protetor solar, não estão a ser suficientes para reverter este problema de saúde pública. Assim sendo, é essencial o desenvolvimento de novas estratégias farmacológicas para a prevenção do CP.

Considerando a importância da p53 mutante na carcinogénese da pele, a reativação de mutantes da p53, através do restabelecimento da sua função nativa, representa uma estratégia promissora na prevenção do CP. Recentemente, o nosso grupo identificou um agente reativador da p53 mutante, o SLMP53-2. A presente tese teve como objetivo avaliar o potencial do SLMP53-2 como agente quimiopreventivo na formação de cancro da pele induzido por radiação UV. Com esse objetivo, efetuou-se o pré-tratamento de queratinócitos humanos com o SLMP53-2, numa dose que não interfere com a proliferação celular, 24 horas antes de exposição das células à radiação UVB. O pré-tratamento com SLMP53-2 aumentou a sobrevivência das células irradiadas. O SLMP53-2 também reduziu a apoptose, a produção de ROS, a inflamação e os danos no DNA, associado a uma regulação das principais proteínas da via NER, tendo ainda aumentado a diferenciação, em células irradiadas com radiação UVB. De forma consistente, a análise *in vivo* revelou uma diminuição na percentagem de células CPD-positivas em ratinhos pré-tratados com SLMP53-2 antes da exposição à UVB, associado a uma indução da via do NER, uma redução na apoptose e inflamação e um aumento da diferenciação.

Em conclusão, os resultados obtidos nesta tese indicam que o composto SLMP53-2 tem uma atividade protetora promissora contra a carcinogénese da pele através da redução dos efeitos nefastos da radiação UVB.

Palavras-chave: Quimioprevenção; Cancro da pele; p53 mutante; Reativação.

Abstract

Skin cancer (SC), including melanoma (MM) and non-melanoma SC (NMSC), is among the most incident type of cancer. Ultraviolet radiation (UVR) constitutes one of the major environmental risk factors associated with SC. Among the major biological effects of UVR that contribute to skin carcinogenesis are DNA damage, particularly the formation of cyclobutene pyrimidine dimers (CPDs) and 6-4 photoproducts (6-4PP), reactive oxygen species (ROS) generation, and inflammation. UVR-induced DNA damage prompts the mutagenesis of important proto-oncogenes and tumor suppressors, such as p53. In fact, *TP53* mutations arise in early stages of skin carcinogenesis and play a crucial role in malignant transformation. The rising incidence of SC indicates that additional preventive strategies against SC development, beyond the use of sunscreen, are required to counteract this public health concern. In particular, the development of novel pharmacological opportunities towards SC prevention would be of high relevance.

Considering the significance of mutant p53 (mutp53) formation in skin carcinogenesis, the reactivation of mutp53, through the reestablishment of its wild-type (wt)-like function, represents a promising strategy of SC prevention. Recently our group identified a new mutp53-reactivating agent, the tryptophanol-derived oxazoloisoindolinone SLMP53-2, with *in vitro* and *in vivo* antitumor activity. In the present thesis, we aimed to evaluate the potential of SLMP53-2 as a chemopreventive agent against UVR-induced SC formation. For that, human keratinocytes were pre-treated with SLMP53-2, at a concentration with no significant effect on cell proliferation, before UVB irradiation. SLMP53-2 increased the survival of UVB-irradiated keratinocytes. The pre-treatment with SLMP53-2 also reduced apoptosis, ROS generation, inflammation and DNA damage, combined with the regulation of major proteins of the NER pathway, while increasing differentiation, in UVB-irradiated cells. Consistently, *in vivo* analysis showed a decrease in the percentage of CPD-positive cells in SLMP53-2-pre-treated mice irradiated with UVB radiation, which was correlated with an induction of the NER pathway, a reduction in apoptosis and inflammation, and increased differentiation.

In conclusion, the results obtained in this thesis indicate that SLMP53-2 has promising protective activity against skin carcinogenesis by reducing the harmful effects of UVB radiation.

Keywords: Chemoprevention; Skin cancer; mutant p53; Reactivation

Table of Contents

Resumo ... 3
Abstract ... 4
Table of Contents ... 5
List of Figures ... 7
Abbreviation list ... 9
Chapter I: Introduction ... 12
1. Introduction to Skin Cancer ... 12
1.1 Epidemiology ... 12
1.2 The Skin structure and cancer subtypes ... 13
1.3 Multifactorial Etiology of Skin Cancer ... 14
1.4 UVR and skin carcinogenesis ... 15
1.5 UVB signaling in carcinogenesis ... 18
2. p53 tumor suppressor protein ... 20
2.1 p53 Protein Structure ... 21
2.2 Regulation by MDMs ... 22
2.3 p53 tumor suppressor functions ... 23
2.3.1 Cell cycle regulation by p53 ... 24
2.3.2 DNA Repair: p53 regulation of the NER pathway ... 25
2.3.3 Apoptosis ... 27
2.3.4 p53 activation and response upon UVR exposure ... 28
2.4 p53 mutations in cancer ... 29
3. Strategies of Skin Cancer Prevention ... 30
3.1 SLMP53-2: A mutp53 Reactivator ... 32
Aims ... 33
Chapter II: Material and Methods ... 34
1. Human cell line and growth conditions ... 34
2. Compounds ... 34
3. Sulforhodamine B (SRB) assay ... 34
4. Trypan Blue Assay ... 34
5. Keratinocyte cells pre-treatment with SLMP53-2 and UVB irradiation ... 34
6. Immunoprecipitation (IP) Assay ... 35
7. Cell Cycle analysis ... 35
8. Western blot analysis ... 36
9. Immunofluorescence (IF) staining ... 38
10. Enzyme-Linked Immunosorbent Assay (ELISA) – TNF-α ... 39

11. Annexin-V assay 39
12. Flow Cytometric analysis of Intracellular ROS 39
13. Slot blot 40
14. Alkaline Comet Assay 40
14.1 Modified Comet Assay 41
15. *In vivo* chemoprevention and toxicity assays 41
16. Immunohistochemistry (IHC) 42
17. TUNEL assay 42
18. Data and statistical analysis 42
Chapter III: Results 44
1. Protective Effect of SLMP53-2 in HaCaT-Irradiated Cells Through Reactivation of Mutp53 44
2. SLMP53-2 Induces Cell Cycle Arrest and Differentiation and Suppresses Inflammation in UVB-irradiated Cells 45
3. SLMP53-2 Protects Against UVB-induced Cell Death with Inhibition of Oxidative Damage 47
4. SLMP53-2 depletes UVB-induced DNA-damage 48
5. *In vivo* protective effect of SLMP53-2 52
Chapter IV: Discussion and Conclusion 57
References 61
Annexes 67

List of Figures

Figure 1 – Incidence and mortality rates of SC types (data from [4]). 12
Figure 2 - The skin structure and skin cell types..... 13
Figure 3 – Major UVR-induced skin damage. 16
Figure 4 – Major UVR-signaling pathways in skin carcingenesis. Black arrows indicate activation. Based on [27]. 19
Figure 5 - p53 structure and the main functions of the p53 domains. On the left, MDM2, a p53 negative regulator, interacts with p53 TAD. On the center, p53 interacts with DNA, through the DBD, as a tetramer. On the right, p53 monomers form a tetramer through interaction of the ODs. PTMs, post-translational modifications. Structures obtained in PDB. PDB codes: MDM2 interaction with p53 derived peptide (1T4F); p53 tetramer bound to DNA (3EXJ); p53 tetramerization (1AIE). 22
Figure 6 – p53 regulation by MDM2 and MDMX..... 23
Figure 7 – Cellular functions of p53 and examples of its target genes involved in each cell process. Vascular endothelial growth factor (VEGF); Thrombospondin-1 (TSP-1); DNA damage regulated autophagy modulator 1 (DRAM1); Protein kinase AMP-Activated non-catalytic subunit beta 1 (PRKAB1); Promyelocytic leukemia protein (PML). 23
Figure 8 - Cell cycle regulation by p53. Arrows indicate activation as opposed to the inhibition arrows. “P” means phosphorylation. Based on [50]. 25
Figure 9 – The NER pathway and its regulation by p53. XPC and DDB2 are transcriptional targets of p53. Based on [53]. 26
Figure 10 – Intrinsic and extrinsic pathways of apoptosis and their regulation by p53. Black arrows indicate induction; Green arrows indicate transcriptional regulation. Based on [55]. 28
Figure 11 – Cellular responses of p53 to UVR. Arrows indicate activation as opposed to the inhibition arrows. Based on [62]. 29
Figure 12 – Chemical structure of SLMP53-2. 32
Figure 13 - SLMP53-2 enhances cell viability of HaCaT irradiated cells through reactivation of mutp53. 44
Figure 14 – SLMP53-2 induces cell cycle arrest and differentiation and suppresses inflammation in UVB-irradiated keratinocyte cells. 46
Figure 15 – SLMP53-2 protects against apoptotic cell death, inhibiting oxidative damage in UVB-irradiated keratinocyte cells. 47
Figure 16 – SLMP53-2 reduces DNA damage in UVB-irradiated keratinocyte cells. 49
Figure 17 - SLMP53-2 protects against UVB-induced CPD and increases the levels of the NER-related proteins XPC and DDB-2. 51

Figure 18 - SLMP53-2 inhibits CPD formation and stimulates NER DNA repair pathway in mice skin. 53
Figure 19 – SLMP53-2 inhibits apoptosis in mice skin 54
Figure 20 - SLMP53-2 inhibits inflammation and promotes differentiation in skin mice. 55

List of Tables

Table 1 - List of antibodies used in western blot (WB), immunohistochemistry (IHQ), immunofluorescence (IF) and slot blot. 36

Abbreviation list

6-4PP – Pyrimidine (6-4) pyrimidone photoproducts

AK – Actinic keratosis

AP-1 - Activator protein 1

ATM - Ataxia-telangiectasia mutated

ATR - Ataxia telangiectasia and Rad3-related

BCC – Basal cell carcinoma

BER – Base excision repair

Cdc25 - Cell division cycle 25 homolog c

CDK - Cyclin-dependent kinase

COX-2 - Ciclo-oxigenase-2

CPD - Cyclobutene pyrimidine dimers

CRD - Disordered regulatory domain

DBD – DNA binding domain

DDB-2 - Damage Specific DNA Binding Protein 2

DMSO - Dimethyl sulfoxide

DSB – Double strand breaks

EGFR – Epidermal growth factor receptor

GADD45 - Growth arrest and DNA damage 45

GOF – Gain of function

JNK - c-Jun N-terminal cinase

LOF – Loss of function

LOH – Loss of heterozygosity

MAPK - Mitogen-activated protein kinase

MDM2 – Murine double minute 2

MDMX – Murine double minute X

MOMP – Mitochondrial outer membrane permeabilization

NER – Nucleotide excision pathway

NF-κB – Nuclear factor kappa-light-chain-enhancer of activated B cells

NMSC – Non-melanoma skin cancer

Nrf-2 - Nuclear factor erythroid 2–related factor 2

PARP - poly(ADP-ribose) polymerase

PCNA - Proliferating cell nuclear antigen

PI3K - Phosphoinositide 3-kinase

PRD – Proline-rich domain

PTCH - Protein patched homolog

Rb - Retinoblastoma

ROS – Reactive oxygen species

SC – Skin cancer

SCC – Squamous cell carcinoma

SSB – Single strand breaks

STAT3 - Signal Transducer And Activator Of Transcription 3

TAD - Transactivation domain

TD – Oligomerization domain

TLS – Translation synthesis

TNF - Tumour necrosis factor

UVR – Ultraviolet radiation

WT – Wild-type

XP - Xeroderma Pigmentosum

XPC - Xeroderma pigmentosum, complementation group C

Part of this work was presented as oral communication at (Annex 1):

SIFFUP 2nd Edition November 24th 2020: Simpósio de Investigação da Faculdade de Farmácia da Universidade do Porto

Rita Ribeiro, Joana B. Loureiro, Nair Nazareth, Tiago Ferreira, Valentina Barcherini, Paula A. Oliveira, Maria M. M. Santos, Lucília Saraiva (2021): SLMP53-2: A Mutant p53 Reactivator With Promising Activity in Skin Cancer Prevention.*

This work was awarded 1st prize at SIFFUP 14th edition.

*Presenting author.

IJUP 14th Edition May 5th 2021 – Encontro de Investigação Jovem da Universidade do Porto

Rita Ribeiro, Joana B. Loureiro, Nair Nazareth, Tiago Ferreira, Valentina Barcherini, Paula A. Oliveira, Maria M. M. Santos, Lucília Saraiva (2021): Chemoprevention of Skin Cancer Through the Mutant p53 Reactivator SLMP53-2.*

This work was awarded best oral communication distinction on the Health Sciences panel at IJUP 14th edition.

*Presenting author.

Chapter I: Introduction

1. Introduction to Skin Cancer

1.1 Epidemiology

Cancer is the second leading cause of death worldwide, with rising incidence and mortality rates that reflect an aging population and stands a barrier for extending life expectancy [1]. In 2020, the Global Cancer Observatory (GCO) estimated 19.3 million new cases and 10 million cancer deaths globally [2]. Importantly, the GCO presents an estimation of a 47% increase of new cancer cases in 2040 relatively to the number of cases reported in 2020 [2].

In particular, skin cancer (SC), including malignant melanoma (MM) and non-melanoma skin cancer (NMSC), is among the most common human malignancy worldwide [3]. According to the World Health Organization, the incidence of NMSC was 1 198 073 cases whereas the incidence of MM was 324 635 cases in 2020 [4]. MM is considered more aggressive compared to the other types of SC, which is mainly attributed to its frequent resistance to therapy and high capacity to metastasize [5]. In fact, MM causes 70% of all SC deaths (Figure 1) [4]. The NMSC subtype includes squamous cell carcinoma (SCC), basal cell carcinoma (BCC), and other rare types of skin cancer [3]. BCC and SCC alone comprise approximately 70% and 25% of all NMSC cases, respectively [6]. Particularly, BCC is the most common and the least aggressive NMSC. On the other hand, SCC is characterized as more aggressive and invasive, causing higher mortality rates than BCC [6]. It is important to mention that NMSC data is somewhat insufficient due to low mortality rates and since the cases may be neglected from cancer statistics. Furthermore, SC incidence also encounters significant geographic variations due to its correlation with sun exposure [7].

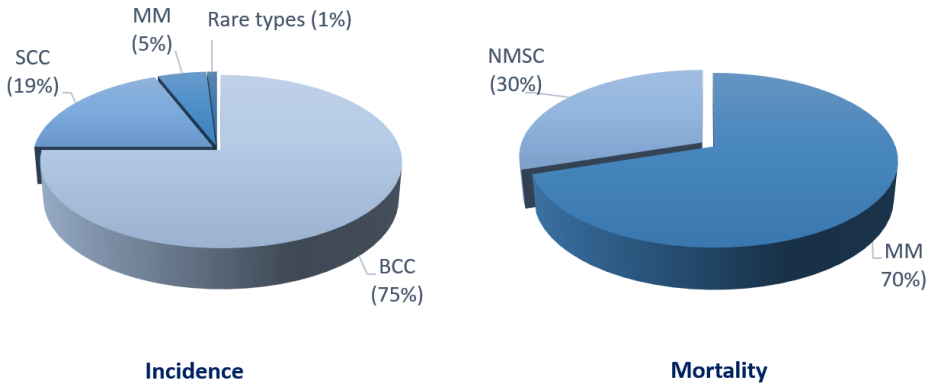


Figure 1 – Incidence and mortality rates of SC types (data from [4]).

1.2 The Skin structure and cancer subtypes

The skin is the largest human organ that works as a physical barrier against thermal and mechanical injuries and as a defense against external pathogens [8]. It is composed of three layers: the epidermis, an outer epithelial layer; the dermis, an inner layer constituted of connective tissue; and the hypodermis, a layer of connective tissue rich in adipocytes (Figure 2). In turn, the epidermis is composed by four layers and four cell types [8]. The deepest layer of the epidermis is called the stratum basale and is separated from the dermis by the basal membrane. This layer is composed by actively proliferating keratinocytes stem cells, that have the capacity to proliferate and produce new keratinocytes [9]. As keratinocytes differentiate, they detach from the basement membrane and migrate towards the surface of the skin [10]. Then, the stratum spinosum is composed by differentiated keratinocytes. Following, it is found the stratum granulosum, where cells lose the nuclei and secrete lipid to intercellular space. The keratinocytes differentiation is also referred to as keratinization, since keratinocytes accumulate keratins which confers distinct structural and functional properties [11]. The most superficial layer is the stratum corneum where keratinized keratinocytes detach from the epidermis [8]. As they migrate towards the surface, basal keratinocytes get flatter and become squamous cells. In the surface, the squamous cells are shedding while new keratinocytes rise from the basal layer [10] (Figure 2).

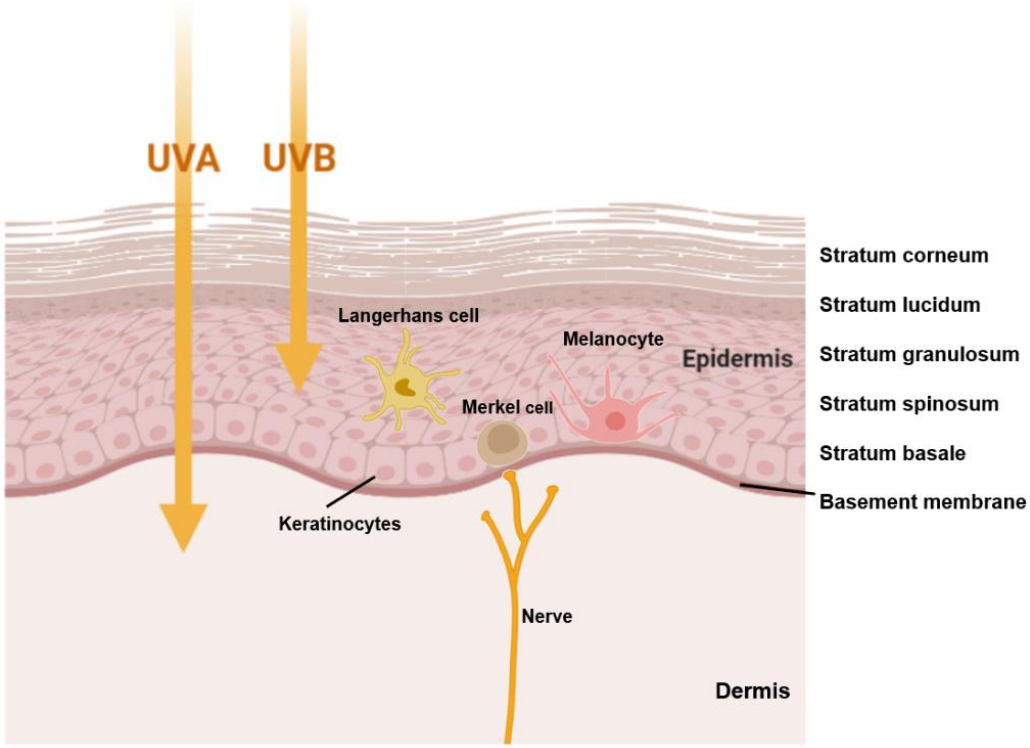


Figure 2 - The skin structure and skin cell types.

The epidermis is constituted by four main cell types, with keratinocytes representing the most predominant type. Melanocytes, melanin-producing cells, also reside in the basal layer. Melanin is stored in adjacent keratinocytes and is crucial in protecting cells from ultraviolet radiation (UVR). Langerhans cells, mainly found in stratum spinosum, are important for the activation of the immune system [12]. Merkel cells, found at the stratum basale, act as mechanosensors in touch-sensitive areas [13] (Figure 2).

SC is categorized depending on the cell type that originates the tumor. For instance, epidermal melanocytes give rise to MM and epidermal keratinocytes originate NMSC [3]. In turn, BCC is originated in keratinocytes from the basal layer of the skin, and SCC is originated in squamous cells from upper layers of the epidermis [3]. Other rare skin cancer subtypes are described, in particular, Merkel cell carcinoma, cutaneous lymphomas, adnexal tumors, among others [7].

1.3 Multifactorial Etiology of Skin Cancer

SC has a multifactorial etiology, including genotypic, phenotypic, and environmental factors, which may differ between the two main types of SC [7].

UVR is among the major environmental risk factors associated with SC [14]. Among NMSC, SCC is the most correlated with UVR [7]. It is well-stablished that phenotypic characteristics such as fair skin, freckles and light-colored eyes and hair, which are considered markers for UVR susceptibility, are associated with an increased risk of NMSC [7]. It is also well-known that NMSC mainly appears in sun-exposed areas and depends on sun exposure and sunburns; thus, it can frequently be reduced by protective measures. Indeed, researchers have concluded that reducing the sun exposure during childhood and adolescence through protective measures could reduce the risk of NMSC up to 78% [12]. Furthermore, people who spend more time outdoors without protective clothing or sunscreen, such as outdoor workers, have increased risk of SC [15]. Specifically, SCC development is more correlated with cumulative/occupational sun exposure, whereas intermittent sun exposure and sun exposure during childhood has been more associated with BCC carcinogenesis [7]. SC incidence also varies geographically, which is associated with variations in solar irradiance when approaching to the equator, providing additional evidence for the relation of SC and UVR [7].

Benign sun-related skin lesions, such as actinic keratoses (AK) and solar lentigines, may evolve to malign lesions [16]. Actinic keratoses (AK) are the most frequent pre-cancerous lesions in human skin and consist of lesions of epidermal keratinocytic dysplasia [16]. AK originate in sun-exposed areas of the skin and result from chronic exposure [16]. AKs are a major health concern due to its high prevalence and risk of progressing to SCC

if not treated [16]. Other environmental factors that increase the risk for NMSC are tobacco smoking, ionizing radiation, arsenic, the use of photosensitizing drugs, infection with HPV, among others [7].

Weakened immune system also constitutes a risk factor, namely in transplantation recipients. Organ transplantation recipients have 65 to 250-fold increased risk of SCC and 16-fold risk of BCC than the general population [7]. The administration of immunosuppressive therapy that enables organ transplantation is in the basis of the increased risk of SC in these cases. [17]. Accordingly, aggressive SCC cases in patients with AIDS or non-Hodgkin lymphoma are also common [7]. Moreover, HPV has an early role in SCC tumorigenesis in immunosuppressed patients. Interestingly, HPV infection can also appear in non-exposed skin to UVR. It is thought that HPV viral proteins facilitate UV-related carcinogenesis through the alteration of cell cycle progression, immune surveillance, and prevention of UV-induced apoptosis and DNA repair [14].

Xeroderma Pigmentosum (XP) is a genetic disorder characterized by failure in DNA repair, specifically in the nucleotide excision repair (NER) pathway, which causes susceptibility to accumulation of UVR-induced damage and further to SC development [18]. This inherited disease reinforces once more the association between UVR and SC. Besides XP, other rarer inherited diseases are coorelated with NMSC susceptibility, which mainly affect the hedgehog pathway genes, namely PTCH1 and PTCH2 [14].

Regarding MM, UVR exposure is also amoung the major risk factors. Furthermore, the number of melanocytic and dysplastic naevi and a personal/family history of MM inscrease its susceptibility [19]. Mutations in the cyclin-dependent kinase inhibitor 2A (CDKN2A) and cyclin-dependent kinase 4 (CDK4) increase the risk of MM and are commonly identified in familial MM [20].

1.4 UVR and skin carcinogenesis

The UV spectrum is the range of the continuous spectrum of electromagnetic radiation that is most relevant in skin damage and carcinogenesis [21]. The sun constitutes the main natural source of UVR; however, man-made devices such as tanning beds and specific working equipment (bactericidal lamps, plasma torches, dental polymerizing equipment, etc) are also relevant sources of UVR. UVR causes harmful health effects, not only taking part in skin carcinogenesis but also in immunosuppression, photoaging, and in other skin diseases. Based on wavelength, UVR can itself be subdivided into ultraviolet A (UVA) 315-400 nm, ultraviolet B (UVB) 280-315 nm, and ultraviolet C (UVC) 100-280 nm [22]. The UVC radiation is the most energetic; however, it is totally absorbed in the ozone layer, thus it does not reach earth's surface. Among the UVR that reaches the earth's

surface, approximately 90-95% is UVA radiation and 5% is UVB radiation [22]. The penetration of UVR on skin depends on its wavelength, thus UVA and UVB have diverse and differentiated effects on skin. Radiation with less energy (with longer wavelengths) can penetrate deeper in the skin. For instance, UVB radiation is more energetic and has less penetration ability, being absorbed mainly by epidermic layers, whereas UVA (less energetic) penetrates deeper, reaching the dermis [22].

The main effects of UVR on skin are the induction of DNA damage, reactive oxygen species (ROS) generation, inflammation, cell signaling alterations, such as the MAPK pathway, and immunosuppression which have a significant role in skin carcinogenesis and photoaging [21] (Figure 3). Particularly, UVB radiation directly induces DNA damage, since it is mainly absorbed by DNA [22], and also triggers ROS generation [22]. UVA radiation is less absorbed by DNA, but it is mainly absorbed by other cell chromophores, also inducing ROS production. ROS can indirectly cause DNA damage through the oxidation of DNA bases [22].

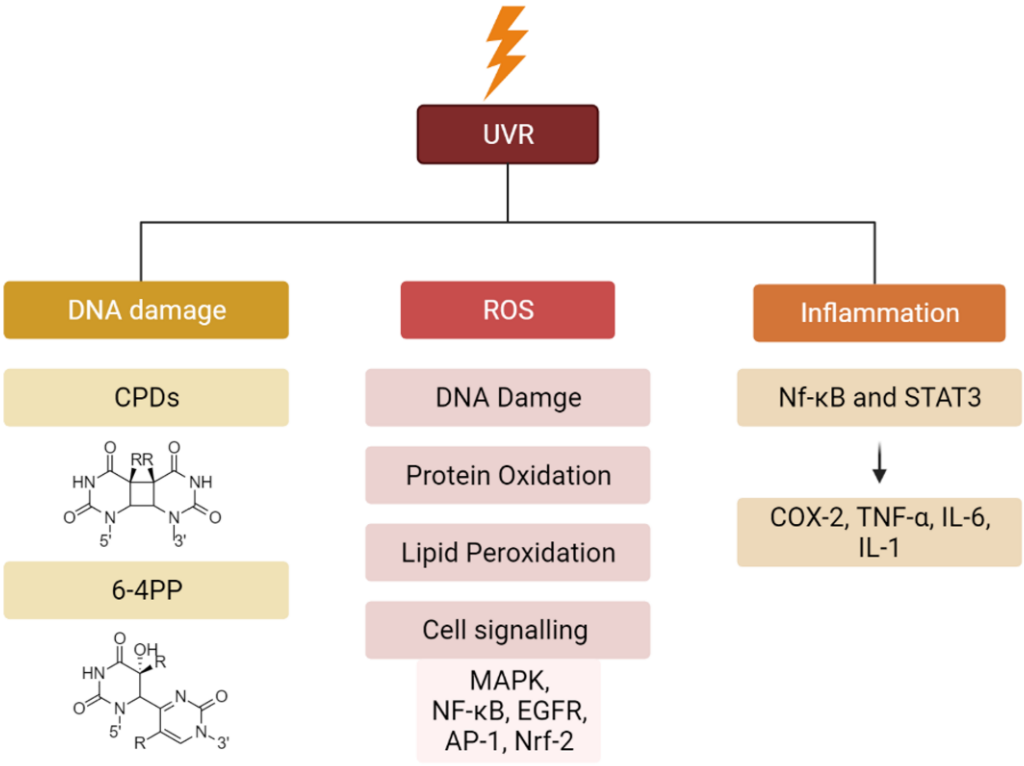


Figure 3 – Major UVR-induced skin damage.

The most frequently observed direct UV-induced DNA lesions are dimeric products, the cyclobutene pyrimidine dimers (CPDs), and pyrimidine (6-4) pyrimidone photoproducts (6-4PPs) (Figure 3), being CPDs 6-fold more common than 6-4PPs [23]. Particularly, CPDs are rapidly formed, within one picosecond of UV exposure, through the cycloaddition of C5-

C6 double bonds of adjacent pyrimidine bases [23]. 6-4PPs are formed by a noncyclic bond between C6 (5'-end) and C4 (3'-end) of two adjacent pyrimidines (Figure 3). This bond leads to an unstable oxetane that by spontaneous rearrangement gives rise to a pyrimidine (6-4) pyrimidone adducts. Subsequently, 6-4PP can photoisomerize into Dewar valence isomers (DewPPs) upon exposure to 320 nm radiation [24]. Both CPDs and 6-4PP create a bulky distortion of the DNA backbone. Besides dimeric products, non-repaired lesions may cause single strand (SSB) and double strand breaks (DBS) in DNA [23]. The extent of DNA damage is determined by several aspects of DNA such as the flexibility of DNA strand, the nature and position of the strand, the state of chromatin and methylation [23].

Considering the role of DNA damage in skin cancer development and since UVB is favorably absorbed by DNA and penetrates epidermic layers, it is considered more carcinogenic. Specifically, UVB radiation is known to favorably induce mutations, which subsequentialy can promote cancer development [23]. Commonly, direct UV-induced lesions are repaired through the nucleotide excision repair (NER) pathway. If the NER pathway fails, the UV-induced lesions may give rise to somatic mutations in S-phase, through a mechanism named error prone translesion synthesis (TLS) [23]. This mechanism allows damaged DNA to replicate without repairing the lesions, leading to mutations that are crucial to cancer initiation. The most common mutations that arise from these UVB-induced lesions are C → T and CC → TT mutations at dipyrimidine sites, designated UV-signature mutations [23].

As previously referred, UVA radiation induces the production of ROS, such as superoxide ($O_2^{\bullet -}$) hydrogen peroxide (H_2O_2) and hydroxyl radical ($^{\bullet}OH$). Excessive levels of ROS after UV exposure lead to cell proliferation, epigenetic alterations, and DNA damage, particularly through the oxidation of DNA bases [23]. Frequent UVA-induced DNA lesions are 8-oxo-7,8-dihydroguanine (8-OxoGua), 8-oxo-7,8-dihydroadenine (8-Oxo-Ade), 2,6-diamino-4-hydroxy-5-formamidoguanine (FapyGua) and 2,6-diamino-4-hydroxy-5-formamidoadenine (FapyAde). Also, ROS may induce the formation of SSB in DNA. The oxidized bases by ROS are normally repaired through the base excision repair (BER) pathway. Defects in this repair pathway also result in the occurrence of somatic mutations. For instance, 8-OxoGua commonly result in G → T mutations. Besides damaging DNA, ROS cause lipids peroxidation and protein carbonylation [25]. Furthermore, ROS regulate signaling pathways involved in carcinogenesis and inflammation, such as the mitogen-activated protein kinase (MAPK) pathway, the nuclear factor kappa-light-chain-enhancer of activated B cells (NF-κB), epidermal growth factor receptor (EGFR), activator protein 1 (AP-1), and nuclear factor erythroid 2–related factor 2 (Nrf-2) [23].

UV-signature mutations are commonly found in proto-oncogenes and tumor suppressors, which explains the importance of these mutations in skin carcinogenesis [26]. Specifically, UV-induced NMSC mainly exhibit UV-signature mutations in the *TP53* gene. In fact, studies have shown that C→T and CC→TT transitions in *TP53* are present in 60-90% of human SCC cases and 50% of all BCC cases [26]. Even though mutant (mut)p53 was found in both SCC and BCC, it is thought that these mutations take part in SCC formation but not in BCC. Instead, mutp53 seems to occur as a second hit during BCC carcinogenesis [27]. Notably, p53 mutations are crucial in early stages of UV-induced skin carcinogenesis. Actually, these mutations were identified in AK lesions, which indicates that mutant p53 appears to have an important role in the conversion of pre-malignant AK lesions to SCC [28]. Continuous UVR exposure promotes the selective clonal expansion of mutp53 keratinocytes. This is possible duo to their resistance to UVR-induced apoptosis and because of their proliferative advantage over wtp53-expressing keratinocytes [28].

1.5 UVB signaling in carcinogenesis

Skin carcinogenesis involves a three-stage process that includes tumor initiation, promotion, and progression [28]. UVR participates in all three stages through the activation of UV-mediated signal transduction pathways [28]. These pathways precede alterations in gene expression that comprise the UV-response in keratinocytes [28].

As previously explained, the tumor initiation by UVR involves irreversible gene mutagenesis in proto-oncogenes and tumor suppressors [23]. During tumor promotion, cells may undergo clonal expansion, in the presence of repeated UVR exposure, causing AK [28]. Tumor promotion involves the induction of MAPK and phosphoinositide 3-kinase (PI3K) pathways, which contribute to AP-1 and cyclooxygenase-2 (COX-2) transactivation [28] (Figure 4). Considering the MAPK pathway activation, UVR is known to induce the activation of p38, extracellular signal-regulated kinase (ERK) and c-Jun N-terminal kinase (JNK) proteins which leads to the activation of AP-1 complex, particularly the c-FOS/JUND dimer, which regulates the expression of genes involved in cell proliferation (Figure 4). In fact, studies have shown that blocking UVB-induced AP-1 activation inhibits skin tumorigenesis [29]. Regarding the PI3K pathway, UVR directly activates PI3K leading to enhancement of c-FOS transcription, and consequently to cell proliferation and survival. [30].

Moreover, the mutagenesis of proto-oncogenes and tumor suppressors, and the constitutive activation of these cell pathways, lead to tumor progression, namely through the conversion of benign AKs to malignant skin tumors [28].

Inflammation occurs as signal-mediated response to UVR exposure and is associated with the different stages of skin tumor development (initiation, promotion, and progression, including invasion and metastasis) [31]. Upon UVR exposure, the transcriptional factors NF-kB and STAT3 are found activated, which regulate the expression of inflammatory regulators, such as IL-1, IL-6 and TNF-α, chemokines, and COX-2 [32].

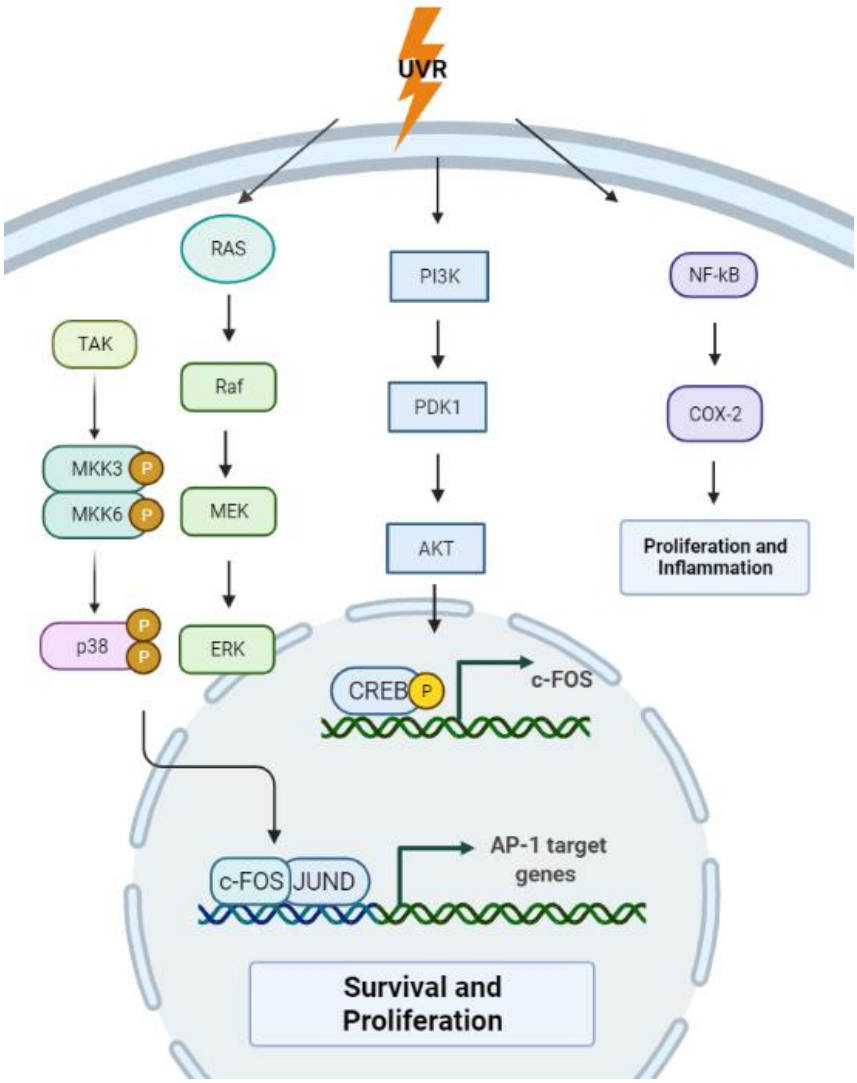


Figure 4 – Major UVR-signaling pathways in skin carcingenesis. Black arrows indicate activation. Based on [27].

2. p53 tumor suppressor protein

As previously refered,*TP53* mutations are commonly present in early stages of skin carcinogenesis as a result of UVR exposure, which makes this protein a relevent target in skin cancer chemoprevention.

The p53 protein, known as guardian of the genome, is codified by the *TP53* gene (located on chromosome 17p13.1) [33]. As a transcriptional factor, p53 regulates the transcription of 500 to 1600 genes, with a decisive role in suppressing tumorigenesis [34].

The p53 protein was discovered in a complex with the simian virus 40 (SV40) large T antigen in 1979 by Professor Sir David Lane. At that time, groups have found a non-viral protein with an apparent molecular mass of about 53 kDa co-immunoprecipitated with SV40, while studying SV40-derived tumor antigens [35, 36]. For several years p53 was thought to be an oncogene as its expression was increased in tumors [37]. Also, it was demonstrated that the overexpression of p53 led to proliferation and an increase in tumorigenicity comparing to p53-null cells [38]. In 1989, p53 was correctly classified as a tumor suppressor and the tumorigenic potential of p53 was explained by the existence of mutant forms of this protein in tumors [39].

In 1997, two p53-related genes, *TP63* and *TP73*, were described [40]. Due to their high level of structural and functional similarity, p63 and p73, together with p53, constitute the p53 family proteins [40]. However, despite these similarities, each protein also exert particular functions. Overall, p63 and p73 cooperate with p53 in the regulation of tumorigenesis, synergistically or in an antagonistic way [40].

p53 acts as a central regulator of cell signaling, which results in the transcription of genes involved in cellular processes such as cell cycle arrest, apoptosis, DNA damage repair pathways, among others [41]. In response to stress stimuli, such as DNA damage, hypoxia, or oncogenic activation, p53 undergoes post-translational modifications that result in its activation, stabilization, and accumulation in the cell, allowing to protect against replication of DNA errors and the proliferation of damaged cells, and also maintaining genome integrity and preventing carcinogenesis [41].

TP53 is the most frequently mutated gene in tumors, with more than 50% of all tumors presenting mutations in this gene [42]. In fact, in these tumors, the p53 signaling pathway is disrupted to enable the proliferation of damage and tumor growth [42].

2.1 p53 Protein Structure

Human p53 protein is found as an homotetramer. Each monomer is composed by 393 aminoacids and incorporates five functional domains [43]. The N-terminal consists of the transactivation domain (TAD), which is divided into two subdomains, TAD1 and TAD2, followed by a proline-rich domain (PRD). The central core of the protein consists of the DNA binding domain (DBD). The C-terminal contains the oligomerization domain (OD) and a disordered regulatory domain (CRD) (Figure 5) [43].

The N-terminal region of p53 is intrinsically disordered which allows interaction with several target proteins with high specificity [44]. The TAD is a protein binding site that establishes multiple interactions important for the transcription activity, for instance, interactions with components of the transcription machinery, coactivators p300 and CBP and p53 negative regulators murine double minute (MDM)2 and MDMX [43] (Figure 5). The activation of p53 depends on the concentration and affinity of regulators that compete for the TAD [44]. Also, this region functions as a display site for post-translational modifications that regulate p53 activity (Figure 5). Upon stress signals, the TAD is modified by post-translational modifications (PTMs), particularly phosphorylations by Ser/Thr kinases, which impar the interaction with negative regulators, such as MDM2 and MDMX, enabling the interaction with coactivators and components of the transcription machinery [43, 44].

The PRD contains five PXXP motifs, which are usually responsible for protein-protein interactions, important in signal transduction [44].

The p53 core domain is natively folded and acquires an immunoglobulin-like β-sandwich structure that acts as a scaffold for DNA binding. p53 binds to DNA through the four DBDs that form the homotetramer [43] (Figure 5). The DBD interacts in a sequence specific manner with DNA in p53-response elements [44]. Thereby, p53 up- or downregulates p53-response elements of target genes, modulating their expression [44].

The OD is required for tetramer formation and, consequently, for p53 activation [45] (Figure 5). As many proteins interact directly with the OD, tetramerization also affects protein-protein interactions. Post-translational modifications may occur in this region and affect the tetramerization and the p53 activity [45].

Likewise the N-terminal, the C-terminal region is intrinsically disordered and may undergo disorder-to-order transition upon protein interaction [44]. The CRD has the capacity to interact non-specifically with DNA, leading to an increase in the stabilization of p53-DNA complex [44]. It is also a site for post-translation modifications, such as acetylation, ubiquitination, phosphorylation, SUMOylation, methylation, and neddylation, which are important in p53 activation, degradation, and localization [43, 44] (Figure 5).

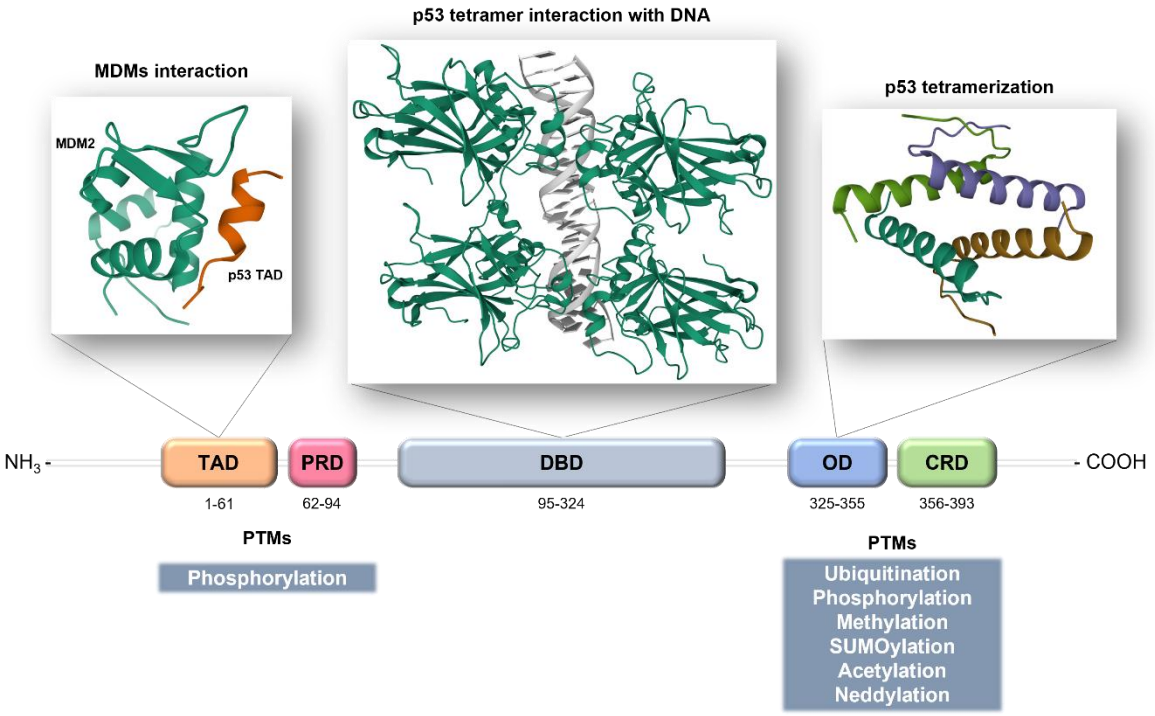


Figure 5 - p53 structure and the main functions of the p53 domains. On the left, MDM2, a p53 negative regulator, interacts with p53 TAD. On the center, p53 interacts with DNA, through the DBD, as a tetramer. On the right, p53 monomers form a tetramer through interaction of the ODs. PTMs, post-translational modifications. Structures obtained in PDB. PDB codes: MDM2 interaction with p53 derived peptide (1T4F); p53 tetramer bound to DNA (3EXJ); p53 tetramerization (1AIE).

2.2 Regulation by MDMs

The p53 activity is regulated by two major negative regulators, MDM2 and MDMX (also referred to as MDM4) [46] (Figure 6). Even though both MDMs are essential for p53 regulation, MDM2 and MDMX have distinct and non-redundant functions [47]. Both MDM2 and MDMX inhibit p53 transcriptional activity through the interaction with p53 TAD [46]. Furthermore, MDM2 promotes the translocation of p53 to the cytoplasm and, as a E3 ubiquitin ligase, it also promotes p53 ubiquitination and its subsequent proteasomal degradation [48]. MDMX, while not having E3 ubiquin ligase activity, cooperates with MDM2 to lead p53 to degradation [48]. In fact, MDM2 and MDMX can form a complex through their RING domains, which stabilizes both proteins and enhances p53 inhibition [46]. In the absence of stress signals, in normal cells, MDM2-MDMX complex binds to and inhibits p53 activity. However, in the presence of damage, MDM2-MDMX complex interaction with p53 is disrupted, releasing p53 from this negative regulation [46] (Figure 6). In fact, upon stress stimuli, MDM2 and MDMX are phosphorylated and their interaction with p53 is disrupted and p53 levels consequently increase [46]. Since MDM2 is a direct transcriptional target of p53, this implicates that activated p53 can upregulate its own inhibitor, which constitutes an

autoregulatory negative feedback loop to restore p53's levels to homeostatic conditions [48].

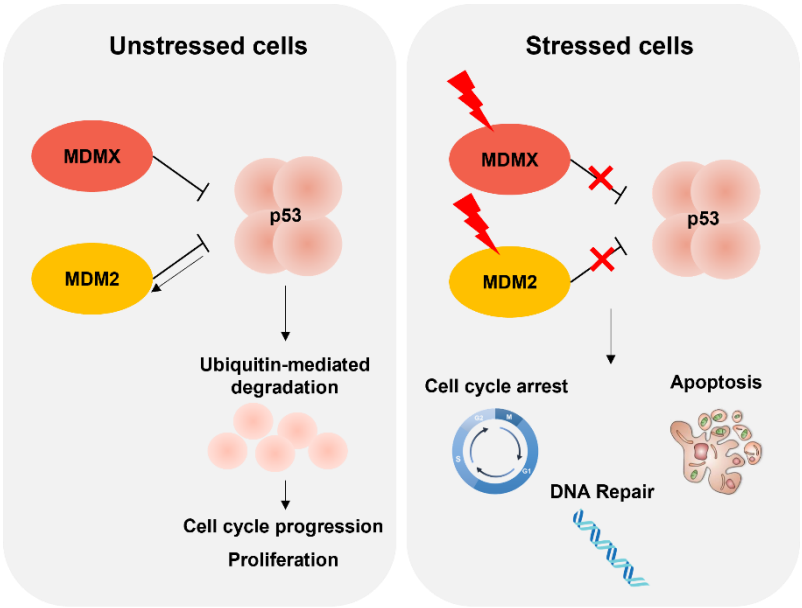


Figure 6 – p53 regulation by MDM2 and MDMX.

2.3 p53 tumor suppressor functions

p53 is responsible for several cellular functions that contribute to tumor suppression, including cell cycle arrest, apoptosis, DNA repair, senescence, differentiation, autophagy, and angiogenesis [49] (Figure 7).

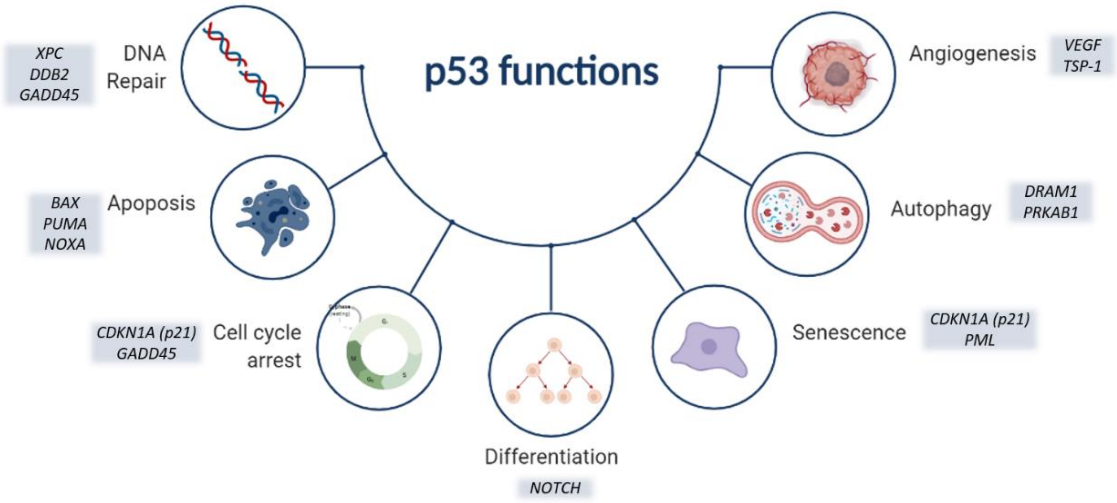


Figure 7 – Cellular functions of p53 and examples of its target genes involved in each cell process. Vascular endothelial growth factor (*VEGF*); Thrombospondin-1 (*TSP-1*); DNA damage regulated autophagy modulator 1 (*DRAM1*); Protein kinase AMP-Activated non-catalytic subunit beta 1 (*PRKAB1*); Promyelocytic leukemia protein (*PML*).

2.3.1 Cell cycle regulation by p53

In the presence of low/moderate stimuli, p53 induces cell cycle arrest. Upon cell cycle arrest, DNA repair mechanisms are activated to repair the damage and protect against transmission of errors to daughter cells [50].

Tumor suppressors, such as p53 or retinoblastoma protein (Rb), sense anomalies and cause cell cycle arrest by regulation of the cyclin-dependent kinases (CDK)-cyclin complexes. The main mechanism whereby p53 mediates cell cycle arrest is through transcription of p21 [50]. p21 interacts with CyclinE/CDK-2 and CyclinD-CDK4 inhibiting them and causing G1-phase arrest [50] (Figure 9). p53 can also lead to G2/M-phase arrest through expression of other target genes such as scaffold protein 14-3-3α, GADD45 with an important role in DNA repair, p21 (inhibits cdk1) and the inhibition of cdc25c necessary for activation of CDK1 [50, 51] (Figure 8).

Cell cycle checkpoints are securely regulated by CDKs, which are Ser/Thr kinases activated by binding with the correspondent regulatory cyclin. The active CDK-cyclin complex phosphorylates proteins involved in DNA replication and mitosis, which causes cell cycle progression. Specific CDK-cyclin complexes regulate the respective phases of the cell cycle, thereby stimulating the correct events and so that its progression occurs sequentially [52].

In the presence of mitogenic signals, quiescent cells enter the cell cycle in G1-phase. This event depends on the increase of the expression of D-type cyclins (D1, D2 and D3) and the formation of their complex with CDK-4 and CDK-6. CyclinD1-CDK4's main function is Rb protein phosphorylation (inactivation). This allows expression of Cyclin E, in turn CyclinE-CDK-2 cooperates in Rb phosphorylation on additional sites. The hyperphosphorylation of Rb disrupts its interaction with E2F proteins in late G1-phase. E2F transcription factor regulates the expression of proteins responsible for DNA replication. E2F has a major role in G1-S transition, and, when overexpressed, allows the entrance of cells in S-phase. Furthermore, G2 progression depends on CyclinB1-CDK1 [50].

In cancer cells, as p53 is commonly altered, the dysregulation of cell cycle allows the division of injured cells, conceding proliferative advantage and accumulation of mutations, which contributes to tumor progression and aggressive phenotypes [42].

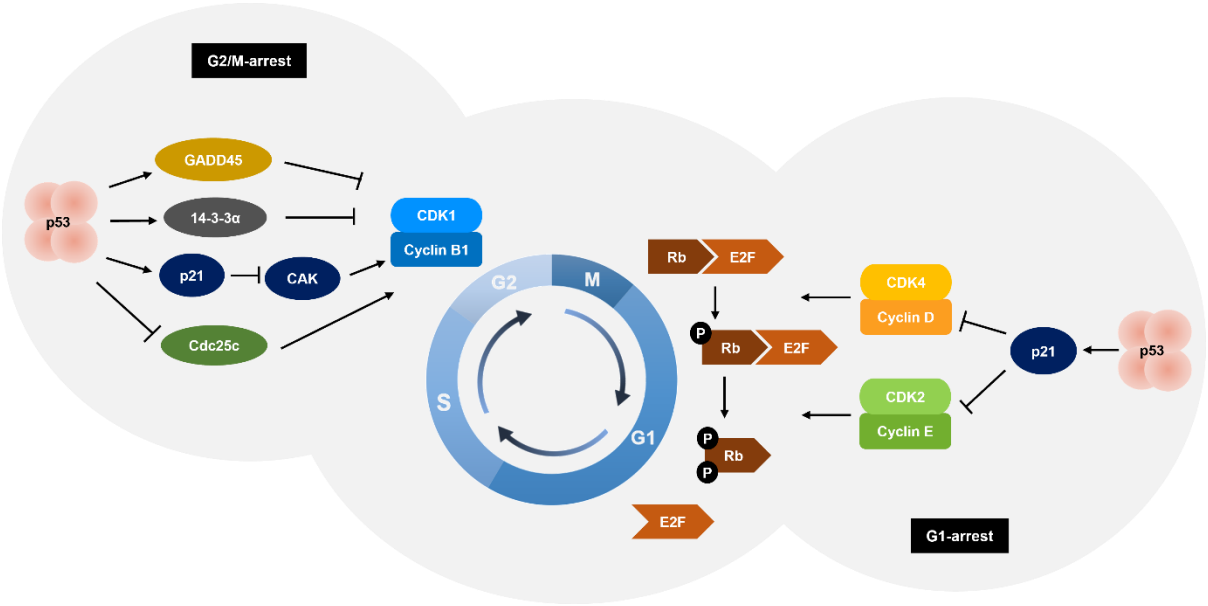


Figure 8 - Cell cycle regulation by p53. Arrows indicate activation as opposed to the inhibition arrows. "P" means phosphorylation. Based on [50].

2.3.2 DNA Repair: p53 regulation of the NER pathway

The involvement in DNA repair is another important function of p53, mainly in the context of SC. Together with the ability to promote cell cycle arrest and apoptosis, p53 induces the repair of UV-induced DNA damage, protecting the genome from damage and avoiding mutagenesis [53].

The NER pathway is one of the DNA repair pathways that removes different types of bulky lesions in the DNA caused by environmental and endogenous factors [54]. In particular, it is responsible for the repair of UVR-induced pyrimidine dimers (CPDs) and 6,4-PP [54]. The NER pathway in subdivided into two pathways which depend on the mode of recognition of the damage. The global genome NER (GG-NER) recognizes damage in the whole genome, whereas the transcription-coupled NER (TC-NER) pathway acts specifically in transcribed strand of actively transcribing genes [54]. In the presence of damage, the RNA polymerase stalls and TC-NER is activated. Both GG-NER and TC-NER require factors for recognition of the damage, in GG-NER pathway these factors are xeroderma pigmentosum (XP) complementation group A (XP-A), XP-C, XP-G, XP-F, replication protein A (RPA), and transcription initiation factor IIH (TFIIH), whereas, in the TC-NER pathway, Cockayne Syndrome group A and B (CSA and CSB) factors, together with RNA polymerase, work in the recognition of the damage. The damage specific DNA binding protein 2 (DDB-2) is an auxiliary recognition factor that directly binds to UV induced lesions and increases the recruitment of XPC to the damage. The repair of the lesion is initiated by

recognition of the damage by components of the NER pathway and progresses through the sequential assembly of other components, such as factors for DNA repair synthesis, proliferating cell nuclear antigen (PCNA), DNA polymerase sigma or ε, and DNA ligase I. XPC initially recognizes the damage, mainly in the case of lesions in the non-transcribing strand. Then, TFIIH complexed with two DNA helicases, XPB and XPD, open the DNA in the site of the lesion (Figure 9). Single strand DNA enables the cleavage by endonucleases. The endonucleases XPG and ERCC1-XPF cleave DNA in the junction between single stranded and double stranded DNA, in the 3' and 5' of the lesion site, respectively. Finally, the oligonucleotide of 24-32 nucleotides is released, and the DNA is synthetized by DNA polymerase [54].

The essential role of NER in maintaining genomic stability is well represented in Xeroderma Pigmentosum (XP). Patients with XP are extremely sensitive to sunlight and have increased susceptibility to SC, mainly due to the inability to repair lesions caused by UVR in skin cells [55].

Upon DNA damage, p53 induces DNA repair by NER pathway through the transcriptional regulation of some genes that encode components of this pathway. The involvement of p53 is restrained to recognition factors of GG-NER, including XPC and DDB-2 [53] (Figure 9).

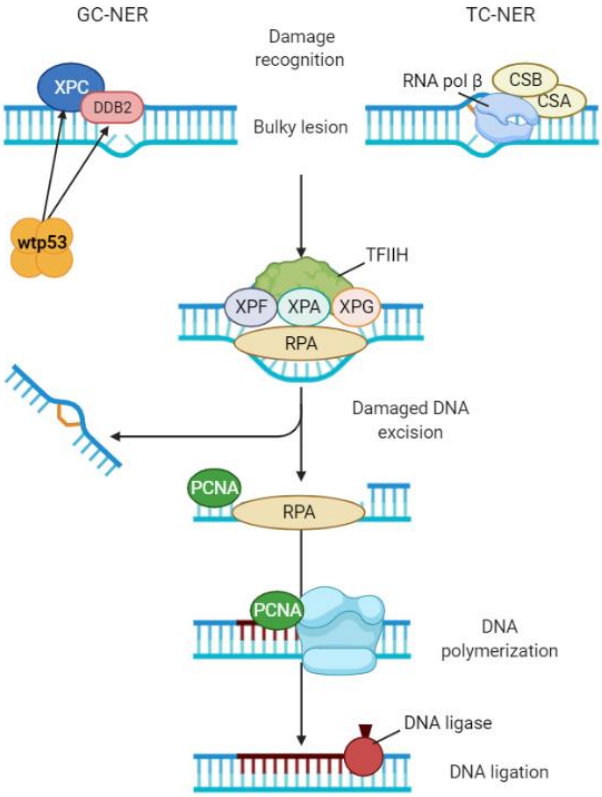


Figure 9 – The NER pathway and its regulation by p53. XPC and DDB2 are transcriptional targets of p53. Based on [53].

2.3.3 Apoptosis

In the presence of severe or irreversible damage, p53 activates apoptosis, a form of programmed cell death, to eliminate damaged cells and avoid oncogenic transformation [56]. Apoptosis can be induced by two distinct mechanisms: the intrinsic or mitochondrial pathway and the extrinsic or death receptor pathway [57].

The first pathway involves the Bcl-2 family proteins that are regulated by tumor suppressor p53 (Figure 10). The Bcl-2 family, composed by 25 genes, includes pro-apoptotic (PUMA, NOXA, Bcl-10, Bax, Bak, Bid, Bad, Bim, Bik, and Blk) and anti-apoptotic (Bcl-2, Bcl-x, Bcl-XL, Bcl-XS, Bcl-W, BAG) proteins [57]. To initiate the pathway, upregulation of pro-apoptotic proteins is required, which mainly induce apoptosis through mitochondrial outer membrane permeabilization (MOMP) and cytochrome *c* (cyt *c*) release. Pro-apoptotic proteins inhibit anti-apoptotic proteins liberating BAX and BAK (apoptosis effectors), which are responsible for mitochondrial permeability transition pore (MTP) formation. Opening of the MTP causes MOMP and loss of transmembrane potential ($\Delta\Psi_m$). The cyt *c* released interacts with APAF1 which results in a conformational change that favors the formation of a complex called the apoptosome, which recruits and activates procaspase 9 [57]. Regarding intrinsic apoptotic pathway induction, p53 has a central role by up-regulating pro-apoptotic proteins such as BAX, PUMA and Noxa [56].

The death receptor pathway depends on the recognition of death ligands (DL) by transmembrane death receptors (DR) on the target cell [57] (Figure 10). Upon binding of the ligand to the receptor, cytoplasmatic adapter proteins, specific of the different DRs, interact with the death domain. For example, for Fas receptor, FADD adapter protein is recruited [57]. Then, the adapter proteins facilitate the interaction of the procaspase 8 to the death-inducing signaling complex (DISC), which causes the dimerization and activation of caspase 8 [57]. Both initiator caspases, caspase 8 or caspase 9 (activated by the intrinsic pathway) further activate executioner caspases (caspases 3, 6 and 7) that promote a cascade of events that result in biochemical changes such as cytoskeleton reorganization and disintegration of the cell into apoptotic bodies [57]. The role of p53 in the extrinsic pathway is due to the transcription of genes encoding components of this pathway, including FAS and other death receptors, sensitizing the cell for the death response [56].

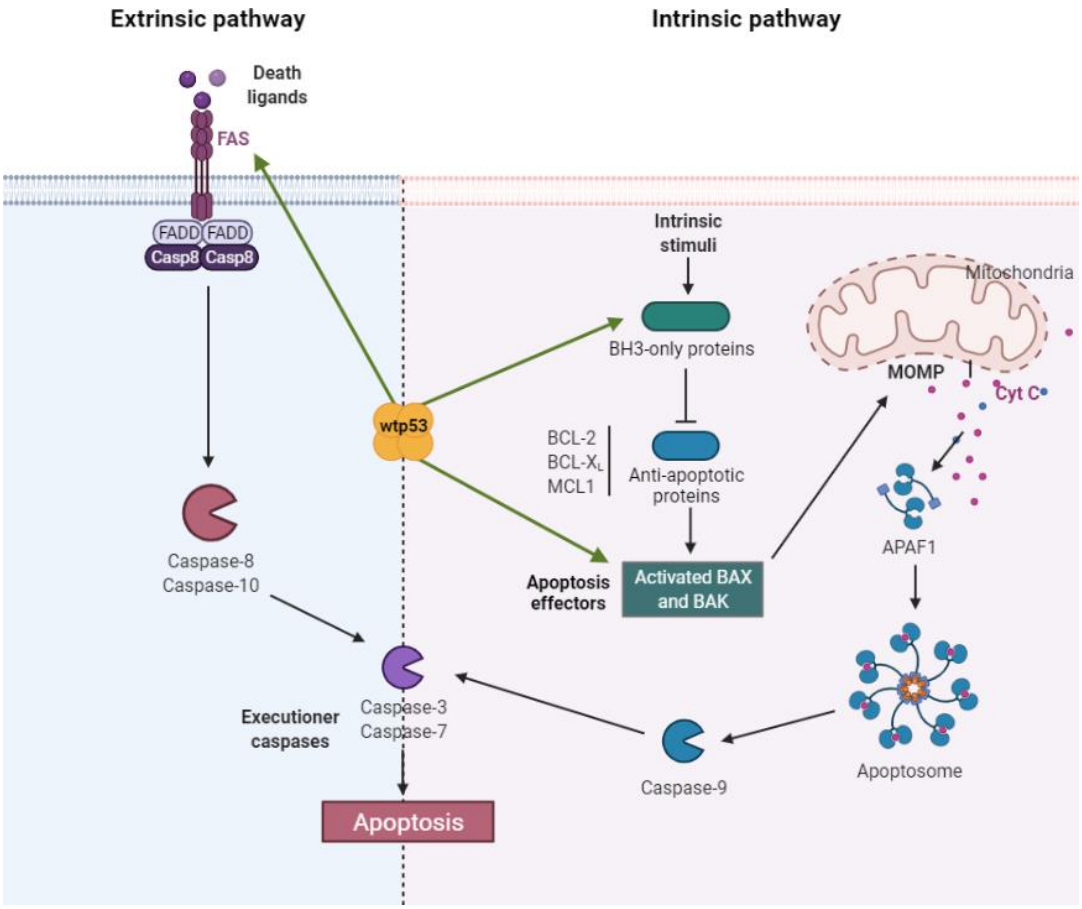


Figure 10 – Intrinsic and extrinsic pathways of apoptosis and their regulation by p53. Black arrows indicate induction; Green arrows indicate transcriptional regulation. Based on [55].

2.3.4 p53 activation and response upon UVR exposure

The p53 tumor suppressor acts as a molecular sensor of UV-induced damage, playing a crucial role in the protection of cells against this damage and eventually carcinogenesis [58]. In non-stressed cells, the p53 levels are kept low; however, after UVR exposure in keratinocytes, p53 accumulates to complete its function [59]. Studies have shown that UVR does not alter *TP53* transcription. Instead, UVR promotes the stabilization of p53, increasing its half-life [60], and its accumulation depends on the type and dose of the stress stimuli [61]. For instance, upon a lower dose of UVR, p53 is transiently induced and promotes cell cycle arrest and DNA repair, in the attempt of correcting the errors [61]. On the contrary, higher doses of UVR lead to a persistent activation of p53, which forces the protein function towards apoptosis induction. In this context, p53 is unable to repair the irreversivel DNA damage, protecting from carcinogenesis through the elimination of damaged cells [61].

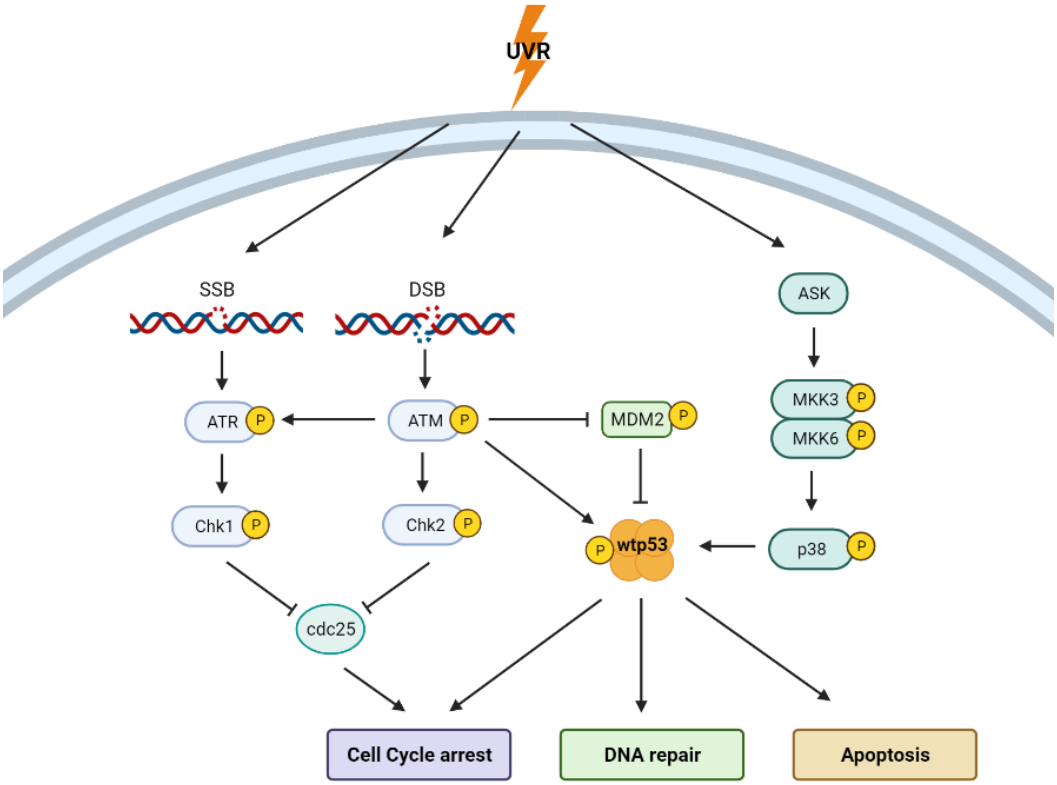


Figure 11 – Cellular responses of p53 to UVR. Arrows indicate activation as opposed to the inhibition arrows. Based on [62].

UVR-induced activation of p53 is also thought to be related with the activation of signaling pathways such as MAPK and ATR/ATM that result in the phosphorylation of p53 serine residues, which is crucial for its accumulation [62]. ATM and ATR are molecular sensors of DNA damage which are activated in the presence of DBS and SSB (Figure 11) [63]. Besides phosphorylation, ATM inhibits MDM2, a negative regulator of p53, by phosphorylation at Ser^{407}, also promoting p53 stabilization [63] (Figure 10). Additionally, ATR and ATM activate Chk1 and Chk2, respectively, which in turn inhibit cdc25 causing cell cycle arrest [27] (Figure 11).

2.4 p53 mutations in cancer

As previosuly refered, over 50% of all human tumors have mutations in the *TP53* gene [42]. Even in tumors that contain wild-type (wt)p53, this gene is normally inactive due to inhibition by its negative regulators, which makes this gene the most frequently altered in human cancers. The relation between p53 mutations and cancer is straightly observed in Li-Fraumeni syndrome, which is a rare hereditary disorder caused by germline mutations in *TP53* that leads to a higher predisposition to cancer development [64].

Regarding the TP53 mutations, the most common are missense mutations that are characterized by a single amino acid substitution. Most of them occur in the DBD, which is a critical domain for p53 activity as a transcriptional factor. In the DBD, six main hotspots have been identified, namely R175, G245, R248, R249, R273 and R282 [65]. p53 mutations can be categorized into structural mutants or DNA contact mutants. Both types of p53 mutations disable its tumor suppressor activity, particularly the DNA binding activity, causing loss of function (LOF). Usually, p53 mutations are followed by loss of the wt allele, with loss of heterozygosity (LOH), and a total disruption of the p53 activity [66].

Furthermore, in heterozygous cells, mutp53 inhibits wtp53 through a dominant negative effect (DNE), causing conversion to a mutant conformation and repression of its wt function. Interestingly, mutp53 may also acquire novel oncogenic functions (gain of function, GOF), which are responsible for a more aggressive phenotype in tumors [65]. Indeed, oncogenic functions of mutp53 include the promotion of proliferation, survival, invasion, migration, angiogenesis, resistance to therapy, among others [65]. In fact, it is known that mutp53 may retain DNA binding activity in mutp53 response elements and not in the standard p53 response elements, leading to alterations in gene expression, sustaining the mutp53 GOF [65]. Also, mutp53 inhibits TAp63/TAp73 activity as tumor suppressors [65].

3. Strategies of Skin Cancer Prevention

Since chronic exposure to UVR represents one of the major risk factors of SC, skin protection against UVR exposure is essential [22]. Particularly, the use of sunscreen is among the main strategies of primary prevention. Also, behavioral practices such as avoiding direct exposure at midday and using appropriate clothing are important [22]. Additionally, self-examination must be done for early detection of skin damage [22].

However, the increasing rates of SC incidence reveal that the mentioned approaches are insufficient [58]. Therefore, the search for improved complementary strategies proves to be crucial. Considering the role of UVR in skin carcinogenesis, namely the UVR-induced DNA-damage, inflammation, ROS production and immunosuppression, it seems relevant to aim at these harmful effects, as a strategy of skin cancer prevention.

Several natural and synthetic compounds with chemopreventive activity against skin cancer development have been described. Generally, these compounds present anti-inflammatory activity, enhancement of DNA repair, ROS scavenging, induction of apoptosis, among others. Additionally, some compounds target UVR-induced signaling pathways that mediate tumor progression, such as the MAPK pathway. Dietary compounds, such as

dietary grape extract, pomegranate, the tea polyphenol epigallocatechin-3-gallate (EGCG) and caffein have shown to inhibit UVR-induced skin carcinogenesis [67-70]

As described previously, UVR-induced mutations in *TP53* arise in early stages of skin carcinogenesis and play an important role in skin cancer development. Therefore, and considering the tumor suppressor functions of this protein, targeting p53 appears to be specially promising in preventing UVR-induced damaging effects and consequently, carcinogenesis. Some compounds have shown to exert its protective activity through the direct or indirect activation of p53 [71-73]. For instance, silibinin, a natural flavonolignan, shows a p53-dependent activity against UVB-induced carcinogenesis, namely through the induction of DNA repair pathways and reduction of UVB-induced inflammatory response [72]. Furthermore, curcumin, another natural compound, protects SKH-1 mice from UVB-induced DNA damage and inhibit UVB-induced proliferation and apoptosis through the induction of p53 [71]. Importantly, oral or topical treatment with this compound, previous to UVB exposure, inhibited tumor multiplicity and delayed tumor onset in SKH-1 mice [71]. Moreover, the synthetic compound CP-31398 revealed to stabilize p53 in its wildtype conformation [74]. Topical administration of this compound on mice's skin, resulted in the activation of p53 target genes, such as p21, MDM2, and PUMA, in UVB-irradiated SKH-1 mice which shows its capacity to restore p53 DNA-binding and transcriptional activity [73]. Notably, CP-31398 inhibits UVB-induced tumor growth in SKH-1 mice [73]. This study reinforces mutp53 reactivation to its wild-type conformation as an encouraging approach to prevent UVR-induced skin cancer [73].

The reestablishment of p53 wt-like conformation by small molecules leads to the restoring of p53 wt-like activity, and consequently, tumor suppression. In the chemoprevention framework, this approach would be promising, not only by the reactivation of preexisting mutations in p53 in the skin but also by the reactivation of UVR-induced mutations. Additionally, the reactivation of mutp53 by small molecules has emerged as a valuable strategy in cancer treatment [75-78]. MANIO and SLMP53-2 (explained in the following subsection) are two mutp53 reactivators identified by our group [75, 76]. MANIO has the capacity to activate wtp53 as well as restore the wt-like function of mutp53 in colorectal cancer (CRC) by direct binding to the DBD [76]. Additionally, the treatment with MANIO lead to the transcriptional regulation of p53 target proteins such as p21, BAX and PUMA. Importantly, in wt- and mutp53-expressing tumors, the compound inhibited tumor proliferation and induced apoptosis. The antitumoral activity of MANIO was validated on patient-derived CRC cells where it shows a significant antiproliferative activity [76].

3.1 SLMP53-2: A mutp53 Reactivator

In a previous work, our group identified the tryptophanol-derived oxazoloisoindolinone SLMP53-2 (Figure 12), as a new mutp53 reactivator [75]. In that work, SLMP53-2 showed potent growth inhibitory effect in hepatocellular carcinoma cells (HCC) expressing mutp53-Y220C through induction of cell cycle arrest, apoptosis, and endoplasmic reticulum stress response. Also, the ability of SLMP53-2 to reactivate mutp53 was demonstrated through enhancement of the mutp53 interaction with the 70-kDa heat shock protein (Hsp70). In particular, SLMP53-2 enhanced the DNA binding ability and subsequent transcriptional activity of mutp53. Furthermore, it was shown that SLMP53-2 was able to reactivate other structural mutp53 such as R175H, -Y220C and -G245S. Importantly, SLMP53-2 presented a potent antitumoral activity in HCC xenograft mouse models with a favorable toxicological profile [75].

More recently, the antitumoral activity of SLMP53-2 against human melanoma cells was also investigated [79]. In that study, the growth inhibitory effect of SLMP53-2 in melanoma cells expressing wtp53 was associated with cell cycle arrest and apoptosis. It was further demonstrated that SLMP53-2 activated wtp53 through the disruption of the p53-MDM2 interaction. Notably, SLMP53-2 also exhibited antitumoral activity in human melanoma xenograft mouse models with no apparent signs of undesirable toxicity [79].

Both studies with SLMP53-2 indicated that this small-molecule has valuable potential as an anticancer agent, not only through the reactivation of mutp53 but also by activating wtp53 in cancer cells. Most importantly, it exhibits high selectivity to tumor cells with a safe toxicity profile.

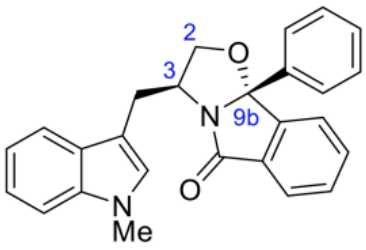


Figure 12 – Chemical structure of SLMP53-2.

Aims

This thesis aimed to evaluate the activity of SLMP53-2 as a chemopreventive agent against skin carcinogenesis. For that, the following goals were followed:

I. Confirmation of mutp53 reactivation by SLMP53-2 in keratinocyte cells;
II. *In vitro* and *in vivo* validation of the protective activity of SLMP53-2 against UVB-induced skin carcinogenesis.

Chapter II: Material and Methods

1. Human cell line and growth conditions

The human keratinocyte HaCaT cell line was purchased from ATCC. Cells were cultured in RPMI-1640 medium supplemented with 10% heat-inactivated fetal bovine serum and incubated in a humidified incubator at 37ºC with 5% CO_2. MycoAlert detection kit was used to assess mycoplasma contamination.

2. Compounds

SLMP53-2 was obtained by synthesis as previously described [75] and dissolved in DMSO (Sigma-Aldrich). For *in vivo* studies, SLMP53-2 was dissolved in acetone.

3. Sulforhodamine B (SRB) assay

Cells were seeded in 96-well plates at a final density of 4.5×10^3 cells/well and incubated for 24 hours. Then, the cells were treated with serial dilutions of SLMP53-2 (3.12-50 µM) and incubated for 24 hours. SBR assay was performed as described [80]. Briefly, cells are fixed with 25 µL 12.5% acid trichloroacetic (TCA) for 1 hour at 4ºC. Then, the cells are washed with dH_2O, dried at room temperature and 50µL 0.4% sulforhodamine in 1% acetic acid solution is added. The plate is incubated for 30 minutes at room temperature and then washed with 1% acetic acid solution. After the plates are dried, 100 µL of 10 mM Tris Base are added and the absorbance is measured at 510 nm. The GI_{10} value (concentration that causes 10% growth inhibition) of SLMP53-2 were determined for the HaCaT cell line using the GraphPad Prism software version 7.0. The solvent of the compound (DMSO) at the maximum concentration used in this assay (0.125%) was included as control.

4. Trypan Blue Assay

The trypan blue assay was done to study cell viability. Cells were seeded in 24-well plates at a final density of 6×10^4 cells/well, incubated for 24 hours and then treated with 3.5 µM SLMP53-2 for 24 hours. After 24 hours of pre-treatment, cells were irradiated with 40 mJ/cm^2 or 80 mJ/cm^2 of UVB radiation and 20 hours after cells were harvested and resuspended in 0.4% Trypan Blue (Sigma-Aldrich). The number of viable or dead cells were counted using a Leica light optical microscope (Wetzlar).

5. Keratinocyte cells pre-treatment with SLMP53-2 and UVB irradiation

The cells were seeded on different plates/flasks and at different densities depending on the experiment, in the previously referred standard conditions, and allowed to adhere for 24

hours. The pre-treatment with the compound SLMP53-2 was performed at a concentration with no significant effect on cell proliferation, corresponding to the concentration that causes 10% growth inhibition, GI_{10} (3.5 µM), for 24 hours. DMSO (vehicle) was used as control.

Following 24 hours of treatment, cells were irradiated with UVB radiation on ice, in the chosen doses, using two UVB lamps in an illuminator equipment (TRIWOOD 31/36, Helios Italquartz, Milan, Italy). For that, the culture medium was removed, and phosphate-buffered saline (PBS) was used (1 mL was used in 6-well plates and 0.5 mL in 24-multiwells) to cover the well's bottom and avoid absorbance of radiation by the medium. The intensity of the radiation was measured with a HD 2302.0 radiometer (Delta OHM, Padova, Italy) with a UVB detector. Non-irradiated control samples were submitted to the same treatment, including PBS treatment, except UVB irradiation. At the end of the irradiation, PBS was replaced for the culture medium without treatment. Finally, the assays were performed in the indicated time-points after UVB exposure.

6. Immunoprecipitation (IP) Assay

For the IP assay, the Pierce Classic Magnetic IP (Thermo Scientific, Dagma, Carcavelos, Portugal) was used. Cells were seeded in flasks at a final density of 5.0×10^5/flask, incubated for 24 hours and then treated with SLMP53-2 for 24 hours. After cell lysis and protein lysate separation, 300 µg of total protein was incubated with 1 µg/mL of mouse monoclonal PAb240 (specific for mut/unfolded p53) or mouse immunoglobulin G (IgG, negative control) from Santa Cruz Biotechnology (Frilabo, Porto, Portugal) for 4 hours at room temperature. The immunoprecipitation of the immunocomplexes was performed using magnetic beads. The western blot analysis was performed, as in Section 2.7., for detection of p53 in the whole cell lysate (input) and in immunoprecipitated proteins (IC). GAPDH was used as a loading control.

7. Cell Cycle analysis

Cell cycle phases were analyzed by flow cytometry. First, cells were synchronized with culture medium without fetal bovine serum (FBS) for 24 hours. After that starvation period, the cells were seeded in 6-well plates at a final density of 1.2×10^5 cells/well and incubated for 24 hours. Then the cells were pre-treated with 3.5 µM SLMP53-2 for additional 24 hours and then irradiated with 40 mJ/cm^2 or 80 mJ/cm^2 of UVB radiation. For cell cycle analysis, cells were stained with propidium iodide (PI) (Sigma-Aldrich). Cell cycle phases were identified and quantified using the FlowJo X 10.0.7 Software (Treestar, Ashland, OR, USA). The AccuriTM C6 flow cytometer and the BD Accuri C6 software (BD Biosciences) were used.

8. Western blot analysis

Cells were seeded in 6-well plates at a final density of 1.2×10^5 cells/well and incubated for 24 hours. Subsequently, cells were pre-treated with 3.5 µM SLMP53-2. After 24 hours of treatment, cells were irradiated with UVB radiation. At 6 hours or 20 hours after irradiation, cells were lysed, whole protein extracts were prepared, and protein expression was evaluated. For whole protein extraction, cells were lysed with radioimmunoprecipitation assay (RIPA) buffer (Sigma–Aldrich, Sintra, Portugal) in the presence of EDTA-free protease inhibitor cocktail (Sigma-Aldrich, Sintra, Portugal). Protein extracts were quantified by the BCA assay using Pierce™ BCA Protein Assay Kit (Sigma–Aldrich, Sintra, Portugal). Protein samples were prepared for loading using SDS-PAGE sample loading buffer and boiled at 95ºC for 5 minutes. Proteins were loaded in 10% SDS-PAGE gel and SDS-PAGE electrophoresis was performed. Then, the proteins were transferred to a Whatman nitrocellulose membrane (Protan, VWR, Carnaxide, Portugal). Membranes were blocked with 5% milk and proteins were detected with mouse monoclonal primary antibodies (Table 1), incubated overnight at 4ºC, followed by an anti-mouse horseradish-peroxidase (HRP)-conjugated secondary antibody, incubated for 2 hours at room temperature. For loading control, membranes were stripped and reprobed with a mouse monoclonal anti-GAPDH antibody. All antibodies were purchased from Santa Cruz Biotechnology (Frilabo, Porto, Portugal). Finally, the signal was detected with the ECL Prime Amersham kit (GE Healthcare, VWR, Carnaxide, Portugal) and the ChemiDoc™ MP Imaging System (Bio-Rad Laboratories, Amadora, Portugal) was used. Band intensities were quantified using the Image Lab software (version 5.2.1; Bio-Rad Laboratories). Signal intensity is relative to the respective loading and normalized to control non-treated cells (Basal), set as 1.

Table 1. List of antibodies used in western blot (WB), immunohistochemistry (IHQ), immunofluorescence (IF) and slot blot.

Antigen	Final Dilution	Supplier
Primary Antibodies		
COX-2 Rabbit polyclonal	1:100 1:100 (IF)	Abcam Cat#ab15191 RRID: AB_2085144
CPD (TDM-2) Mouse monoclonal	1:100 (IHQ) 1:100 (IF)	Cosmo Bio Co., LTD Cat# CAC-NM-DND-001; RRID: AB_1962813

Cytokeratin 1 (4D12B3) Mouse monoclonal	1:500 1:40 (IHQ)	Santa Cruz Biotechnology Cat# sc-65999; RRID: AB_2234496
Cytokeratin 10 (RKSE60) Mouse monoclonal	1:100	Santa Cruz Biotechnology Cat# sc-23877; RRID: AB_2134668
DDB-2 (D4C4) Rabbit monoclonal	1:300 (WB) 1:100 (IHQ)	Cell Signaling Cat# 5416; RRID: RRID: AB_10694497
DNP Rabbit polyclonal	1:5000	Merck Millipore Cat# D9656; RRID: AB_259258
GAPDH (6C5) Mouse monoclonal	1:10000	Santa Cruz Biotechnology Cat# sc-32233; RRID: AB_627679
IL-6 (1.2-2B11-2G10) Mouse monoclonal	1:100 1: 100 (IF)	Abcam Cat#ab9324; RRID: AB_307175
Involucrin (SY5) Mouse monoclonal	1:500 1:100 (IHQ)	Santa Cruz Biotechnology Cat# sc-21748; RRID: AB_2128119
JNK (EPR16797-211) Rabbit monoclonal	1:5000	Abcam Cat# ab179461; RRID: AB_2744672
NF-kB p65 (A-12) Mouse monoclonal	1:1000 (WB) 1:80 (IF)	Santa Cruz Biotechnology Cat# sc-514451; RRID: AB_2891257
Nitro-tyrosine Rabbit polyclonal	1:1000	Cell Signaling Cat# 9691; RRID: AB_331634
NOTCH-1 (A-8) Mouse monoclonal	1:100	Santa Cruz Biotechnology Cat# sc-376403; RRID: AB_11149738
PARP (C2-10) Mouse monoclonal	1:100	Santa Cruz Biotechnology Cat# sc-53643; RRID: AB_785086
p-JNK (EPR5693) Rabbit monoclonal	1:1000	Abcam Cat# ab124956; RRID: AB_10973183
p21 (F-5) Mouse monoclonal	1:100	Santa Cruz Biotechnology Cat# sc-6246; RRID: AB_628073
p53 (DO-1) Mouse monoclonal	1:5000 (WB)	Santa Cruz Biotechnology Cat# sc-126; RRID: AB_628082
p53 (PAb 240; Ab-3) Mouse monoclonal	1:50 (IP) 1:20 (IHQ)	Merck Millipore Cat# OP29; RRID: AB_10683190
p-γH2AX (S139) Rabbit polyclonal	1:500	Abcam Cat# ab2893; RRID: AB_303388
XPA (B-1) Mouse monoclonal	1:200	Santa Cruz Biotechnology Cat# sc-28353; RRID: AB_628450

XPC (3.26) Mouse monoclonal	1:100 (WB) 1:80 (IHQ)	Thermo Fisher Scientific Cat# MA1-23328; RRID: AB_561968
4-Hydroxynonenal Goat polyclonal	1:1000	Merck Millipore Cat# AB5605; RRID: AB_569332
Secondary antibodies		
Alexa Fluor 488 Anti-mouse IgG	1:100 (IF)	Thermo Fisher Scientific Cat# A11001; RRID: AB_2534069
Alexa Fluor 488 Anti-rabbit IgG	1:100/1:400 (γ-H2AX) (IF)	Thermo Fisher Scientific Cat# A11008; RRID: AB_143165
Anti-mouse HRP-conjugated	1:5000	Abcam Cat# ab6789; RRID: AB_955439
Anti-rabbit HRP-conjugated	1:5000	Abcam Cat# ab6721; RRID: AB_955447
Anti-rabbit HRP-conjugated	1:5000 (Slot-blot)	Merck Millipore Cat# AP307P; RRID: AB_11212848
Anti-goat HRP-conjugated	1:5000 (Slot-blot)	Merck Millipore Cat# AP107P; RRID: AB_11214432

9. Immunofluorescence (IF) staining

The immunofluorescence staining was used for the analysis of several markers, including H2AX histone. HaCaT cells were seeded in round cover slides in 24-well plates at a final density of 6×10^4 cells/well and incubated for 24 hours. Cells were pre-treated with 3,4 µM SLMP53-2. After 24 hours of treatment, cells were irradiated with UVB radiation (40 mJ/cm^3 and 80 mJ/cm^3). Then, cells were fixed with 4% paraformaldehyde solution for 15 minutes at room temperature, followed by permeabilization with 0.5 % Triton X-100 in PBS solution during 15 minutes on ice. For CPD analysis, 2M HCl was used to denature cellular DNA, for 30 minutes. Cells were then blocked for 30 minutes using 20% FBS in PBS solution, to prevent non-specific antibody binding. Primary antibodies (Table 1) were incubated for 2 hours. Fluorochrome conjugated secondary antibody, AlexaFluor 488 anti-Mouse, was incubated for 1 hour at room temperature. Finally, DAPI (40 ,6-Diamidino-2-Phenylindole, dihydrochloride) (0.1 µg/mL) was used as a nuclear counterstain to reveal all cells and the slides were mounted with Vectashield mounting medium (Vector, Batista Marques, Lisboa, Portugal) and kept at 4°C until analysis. Images were acquired with fluorescence microscope a Nikon eclipse Ts2R-C-AL microscope with a Nikon LV-TV

camera, and NIS Elements BR-5.20 software (Nikon Corporation). Collected images were generated using Fiji software, also used for quantifications.

10. Enzyme-Linked Immunosorbent Assay (ELISA) – TNF-α

The ELISA assay was used to measure TNF-α protein levels in the culture medium. For this purpose, HaCaT cells/well were seeded in 6-well plates at a final density of 1.2×10^5 cells/well for 24 hours, followed by a pre-treatment with SLMP53-2 for 24 hours. After 24 hours, cells were irradiated with UVB radiation and, 20 hours after, the concentrations of the pro-inflammatory cytokine TNF-α were determined in the supernatants using an ELISA MAX Deluxe kit, according to the manufacturer's instructions (BioLegend Inc.; San Diego, CA, USA). Briefly, a capture TNF-α specific antibody is precoated in 96-well plates and the samples are incubated to allow antibody-antigen interaction. Then, the detection TNF-α specific antibody, is added, forming a "sandwich", followed by the addition of HRP enzyme. Finally, a substrate solution for HRP is added to produce a measurable colorimetric signal.

11. Annexin-V assay

The quantification of apoptotic cells was done using the annexin-V assay. This assay is based on the cell staining with FITC-labelled Annexin-V and PI. Annexin-V binds to phosphatidylserine (PS) which is a phospholipid exposed during apoptosis and PI is used for DNA staining. This way we can identify intact cells ($FITC^-/PI^-$) and apoptotic cells, in early ($FITC^+/PI^-$) or late ($FITC^+/PI^+$) apoptosis [81].

For that, 1.2×10^5 HaCaT cells/well were seeded in 6-well plates and allowed to adhere overnight. Then, HaCaT cells were treated with SLMP53-2 for 24 hours, irradiated with UVB radiation and collected for analysis 10 hours after. Finally, cells were stained using the Annexin V-FITC Apoptosis Detection Kit I from BD Biosciences (Enzifarma, Porto, Portugal), according to the manufacturer's instructions, and analyzed by flow cytometry. The AccuriTM C6 flow cytometer and the BD Accuri C6 software (BD Biosciences) were used.

12. Flow Cytometric analysis of Intracellular ROS

HaCaT cells were seeded in 6-well plates at a final density of 1.2×10^5 cells/well and incubated for 24 hours. Cells were pre-treated with SLMP53-2 and, after 24 hours of treatment, cells were irradiated with UVB radiation ($80 mJ/cm^2$). Finally, cells were harvested and stained with 10 µL of H2DCFDA (2′,7′- dichlorofluorescin diacetate) probe, which detects general oxidant levels in the cell [82], at a final density of 10 µM in complete medium at 37°C, 5% CO_2 for 30 min. The cells were finally analyzed by flow cytometry, using the

FlowJo X 10.0.7 Software (Treestar, Ashland, OR, USA). The AccuriTM C6 flow cytometer and the BD Accuri C6 software (BD Biosciences) were used.

13. Slot blot

Slot blot assay was used to measure the carbonyl and nitrotyrosin groups and of 4-hydroxynonenal levels. For that, 1.2×10^5 HaCaT cells/well were seeded in 6-well plates for 24 hours, followed by a pre-treatment with SLMP53-2 for 24 hours. After the pre-treatment, cells were irradiated with the indicated dose of UVB radiation. For determination of nitrotyrosin and 4-hydroxynonenal levels, 5 µg of protein were diluted in PBS. Protein carbonyl group levels were derivatized. For that, a 12% SDS solution was added followed by 20 mM 2,4-dinitrophenylhydrazine (DNPH) in 10% trifluoracetic acid (TFA). The samples were incubated at room temperature protected from light for 15-30 minutes. Finally, Tris 2M with 18% β-mercaptoetanol as a stop solution was added. The prepared proteins were then transferred to polyvinylidene difluoride membranes using a Hybri-slot manifold system (Biometra). Then, membranes were blocked and incubated with the respective primary antibodies (Table 1) overnight at 4° C. After incubation with secondary antibodies, membranes were reacted and visualized with ECF detection system (GE Healthcare) and visualized with the BioRad GelDoc XR (Bio-Rad). The densities from each band were obtained using the Quantity One software (Bio-Rad).

14. Alkaline Comet Assay

The alkaline Comet assay, also referred to as single cell gel electrophoresis (SCGE) was performed with the goal of evaluating DNA damage. For that, 1.2×10^5 HaCaT cells were seeded on 35 mm Petri dishes, treated 24 hours with SLMP53-2, and immediately after UVB irradiation of cells, comet assay was executed. To perform the experiments, cells were collected, mixed with 0.5% of LMA (Low Melting Agarose) and then seeded on agarose-coated slides. Then, another layer was spread and left 10 minutes a 4ºC for solidification. Later, slides were soaked in a lysis solution (10% DMSO, 1% Triton X-100, 89% Stock solution: 2.5 M NaCl, 250 mM NaOH, 100 mM Na_2EDTA, 10 mM Tris in water, pH 10; Sigma Aldrich) for 30 minutes at 4°C. Subsequently, slides were neutralized (0.4 M Tris, pH 7.5) and then kept for 30 minutes in stabilization inside an electrophoresis system with an alkaline buffer (300 mM NaOH, 1 mM Na_2EDTA in water, pH>13), for DNA unwinding. At the end of the stabilization, the electrophoretic run was performed for 30 minutes, at 300 mA and 25V. Slides were neutralized again and stained with PI and analyzed by fluorescence microscopy (40× oil objective). A total of 100 cells/sample was

analyzed using software (TriTek CometScore™).

14.1 Modified Comet Assay

A modified Comet assay using the T4-endonuclease enzyme was performed to evaluate specifically UVB-induced DNA damage. This protocol is similar to the alkaline comet assay except for some modifications. The pH of the alkaline buffer was set to 12.1; after the lysis, slides were incubated for 45 minutes at 37ºC with 50 µL of the diluted enzyme T4 PDG (New England BioLabs® Inc.), allowing the cleavage of pyrimidine dimers. The enzyme was then diluted in T4 PDG Reaction buffer at a final concentration of 10 U/mL, according to manufacturer's instructions.

In fact, the level of fragmented DNA increases in the modified comet assay compared to the comet assay without T4-endonuclease for the same experimental conditions [83]. Regarding the analysis of the results, these are presented as percentage of nucleoids type (A nucleoids, BCD, and E nucleoids), tail length, percentage of DNA in the comet tail and tail moment. The nucleoids consist in DNA attached to residual proteins insensitive to the lysis process and their classification is based on the tail moment parameter, for instance, type A nucleoids contain undamaged DNA whereas type E nucleoids contain completely damaged DNA [84]. Finally, the tail moment is defined as the product of tail length and the percentage of DNA in the comet tail [84].

15. *In vivo* chemoprevention and toxicity assays

All the *in vivo* procedures were approved by the University of Trás-os-Montes and Alto Douro Ethics Committee (10/2013) and the Direção Geral de Alimentação e Veterinária. The animals were kept under controlled conditions of temperature (23 ± 2°C), light-dark cycle (12 hours light/12 hours dark), and relative humidity (50 ± 10%).

For the *in vivo* studies, 13-weeks-old female FVB/N mice were used and randomly divided into 4 groups of 5 mice: non-irradiated control, UVB-irradiated control, SLMP53-2 treated, and SLMP53-2 pre-treated and UVB irradiated. A dorsal trichotomy was performed to expose the skin to UV radiation using a shaving machine.

Pre-treatment with 1.5 mg SLMP53-2 in 200 µL acetone was topically applied 1 hour before UVB irradiation. Mice were dorsally irradiated using the equipment TRIWOOD 31/36 Helios Italquartz after sedation with isoflurane. After 24 hours of irradiation, mice were sacrificed and the irradiated portion of skin was removed. For toxicity assays, female mice were treated with SLMP53-2 or vehicle (DMSO) twice a week for 2 weeks.

16. Immunohistochemistry (IHC)

IHC analysis was performed in mice skin. Dorsal skin was fixed in 10% formalin, embedded in paraffin, sectioned, and stained with hematoxylin and eosin (H&E) or antibodies. Briefly, after deparaffination and rehydration, antigen retrieval was performed by boiling the sections for 20 minutes in 10 mM citrate buffer (pH 6.0). The slices were then held for 20 minutes at room temperature. Endogenous peroxidases were blocked using with UltraVision Hydrogen Peroxide Block and proteins were blocked with UltraVision Protein Block solution, both from Lab Vision Thermo Scientific. Incubation with primary antibodies (Table 1) was performed for 2 hours, at room temperature. Immunostaining was carried out using the UltraVision Quanto Detection System HRP DAB kit, from Lab Vision Thermo Scientific. Finally, tissues were counterstained with hematoxylin, clarified, dehydrated, and mounted. For IF staining, after antigen retrieval, the slides were incubated with primary antibody overnight at 4ºC, following incubation with Alexa Fluor 488-conjugated secondary antibody for 2 hours at room temperature, and stained with DAPI.

Evaluation of DAB (3,3′-diaminobenzidine) intensity, quantification of stained cells in mouse epidermis, and the determination of mean fluorescence were performed using ImageJ software version 1.8.0. (Madison, WI, USA). Images from IHQ were obtained using an Eclipse E400 fluorescence microscope (Nikon) with 200× magnification, with a Digital Sight camera system (Nikon DS-5Mc) and software Nikon ACT-2U (Izasa). Images from IF were obtained from a Nikon eclipse Ts2R-C-AL microscope with a Nikon LV-TV camera, and NIS Elements BR-5.20 software (Nikon Corporation).

17. TUNEL assay

TUNEL assay enabled us to analyze the formation of DNA fragments during apoptosis, using the in-situ Cell Death Detection Kit Fluorescein from Roche, according to the manufacturer's instructions. After deparaffination and rehydration, tissues sections were treated for 20 minutes in 10 mM citrate buffer (pH 6.0) and incubated with TUNEL Reaction Mixture for 60 minutes at 37°C in the dark. Tissues were counterstained with DAPI (0.1 µg/mL). Images were obtained using an Eclipse E400 fluorescence microscope (Nikon), 400× magnification, with a Digital Sight camera system (Nikon DS-5Mc), carrying built-in software for image acquisition (Nikon ACT-2U).

18. Data and statistical analysis

Data were statistically analyzed using the GraphPad Prism software v7.0 (GraphPad Inc., La Jolla, CA, USA). The results were analyzed using ANOVA *t*-test to assess statistical significance, two-way ANOVA analysis followed by post-hoc Bonferroni tests for multiple

comparisons, one-Way ANOVA Tukey's multiple comparisons test and one-Way ANOVA test, Dunnett's multiple comparison test. Results were considered statistically significant at $p < 0.05$.

Chapter III: Results

1. Protective Effect of SLMP53-2 in HaCaT-Irradiated Cells Through Reactivation of Mutp53

The effect of SLMP53-2 was studied in the human keratinocyte HaCaT cell line, expressing two-point mutations in *TP53* (codon 179 of exon 5 and codon 282 of codon 8). The SRB assay was performed to determine the non-cytotoxic concentration of SLMP53-2, in these cell lines (Figure 13A). The results showed a no significant growth-inhibitory effect of SLMP53-2 at 3.5 μM (GI_{10} value). We next evaluated the effect of the pre-treatment of the cells for 24h with 3.5 μM SLMP53-2 in cell viability of keratinocyte cells irradiated with 40 or 80 mJ/cm^2 of UVB radiation by trypan blue assay (Figure 13B). The results evidenced a significant reduction in cell viability, compared to the non-irradiated control (DMSO), for both doses of UVB radiation. Importantly, 3.5 μM SLMP53-2 increased cell viability for 40 or 80 mJ/cm^2 of UVB radiation compared to the DMSO-only treated cells. In the non-irradiated controls, SLMP53-2 or DMSO did not infer with cell viability. To further understand the potential molecular mechanism underlying this effect, we investigated the effect of SLMP53-2 in the levels of mutp53, in HaCaT cells before UVB exposure, through the immunoprecipitation of p53 with PAb240, a conformation-specific antibody for mutp53 forms (Figure 13C). As expected, the pre-treatment for 24h of keratinocyte cells with 3.5 μM SLMP53-2 reduced the levels of immunoprecipitated mutp53, without affecting the total amount of p53, when compared to the nontreated samples. These results indicated the reactivation of mutp53 by SLMP53-2, in HaCaT cells.

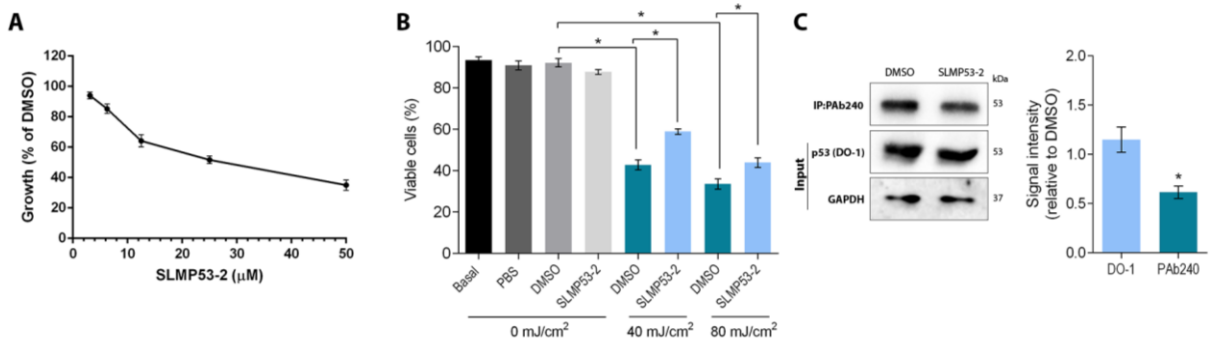


Figure 13 - SLMP53-2 enhances cell viability of HaCaT irradiated cells through reactivation of mutp53.
(A) Concentration-response curves for SLMP53-2 in HaCaT cells, analyzed by SRB assay after 24 h of treatment with 3.12–50 μM SLMP53-2. Data are mean ± SEM (n = 5). **(B)** Effect of 3.5 μM SLMP53-2 on cell viability determined by trypan blue assay 20 h after UVB for 40 and 80 mJ/cm^2. Data are mean ± SEM of 4 independent experiments. Values significantly different from DMSO (non-irradiated control): *p < 0.05 (One-Way ANOVA test, Dunnett's multiple comparison test), and from DMSO treated cells irradiated *p < 0.05 (One-Way ANOVA Tukey's multiple comparisons test). **(C)** Immunoprecipitation assay was performed in HaCaT cells treated with 3.5 μM SLMP53-2 for 24 h, using PAb240 antibody. p53 from input (whole cell lysate)

was used as loading control. Quantification of protein expression levels relative to DMSO (set as 1). Data shown are means ± SEM, of 4 independent experiments.

2. SLMP53-2 Induces Cell Cycle Arrest and Differentiation and Suppresses Inflammation in UVB-irradiated Cells

Considering the crucial role of p53 in the suppression of skin carcinogenesis, the effect of SLMP53-2 pre-treatment on cellular processes regulated by p53, including cell cycle, inflammation, and differentiation, was studied.

We first analysed the effect of 3.5 μM SLMP53-2 pre-treatment on cell cycle progression of 40 and 80mJ/cm^2 of UVB radiation-exposed HaCaT cells. The results showed a G1-phase cell cycle arrest induced by 40 mJ/cm^2 of UVB radiation. Furthermore, for 80 mJ/cm^2 UVB radiation there is a mild increase in S-phase, which is frequently associated with replicative stress, as a consequence of DNA damage. This result is, actually, in accordance with our data from apoptosis analysis, since 80 mJ/cm^2 radiation led to a significance induction of apoptosis. Moreover, although the treatment with 3.5 μM SLMP53-2 did not interfere with the effect obtained with 80 mJ/cm^2, it increased the G1-phase cell cycle arrest in 40 mJ/cm^2 irradiated cells (Figure 14A). Consistently, it also increased the levels of p21, a cell cycle regulator, in 40mJ/cm^2 irradiated cells, when compared to DMSO (Figure 14 2B).

We next studied the impact of SLMP53-2 pre-treatment in the inflammation process through the analysis of the expression levels of inflammatory markers. By immunofluorescence assay, it was observed that 40mJ/cm^2 of UVB radiation induced the translocation of NF-κB (p65 subunit) to the nucleus (Figure 14C), which was significantly reduced by pre-treatment with 3.5 μM SLMP53-2 (Figure 14C). By western blot, it was also verified an increase of NF-κB, COX-2 and IL-6 protein levels, in the irradiated cells compared to non-irradiated samples, which was decreased in the 3.5 μM SLMP53-2 pre-treated cells (Figure 14E). Furthermore, a major increase in the levels of secreted TNF-α, another inflammatory mediator, was induced by 40mJ/cm^2 UVB radiation, which was significantly decreased by 3.5 μM SLMP53-2 pre-treatment (Figure 14F).

Regarding cell differentiation, we observed an induction of involucrin, cytokeratin 1 (K1) and cytokeratin 10 (K10) and a reduction of NOTCH-1 caused by 40mJ/cm^2 UVB radiation. Moreover, 3.5 μM SLMP53-2 pre-treatment increased the protein levels of K1, K10, involucrin and NOTCH-1 when compared to the irradiated control (Figure 14G).

Altogether, these results indicated that SLMP53-2 protects keratinocytes from UVB-induced inflammation, while stimulating differentiation.

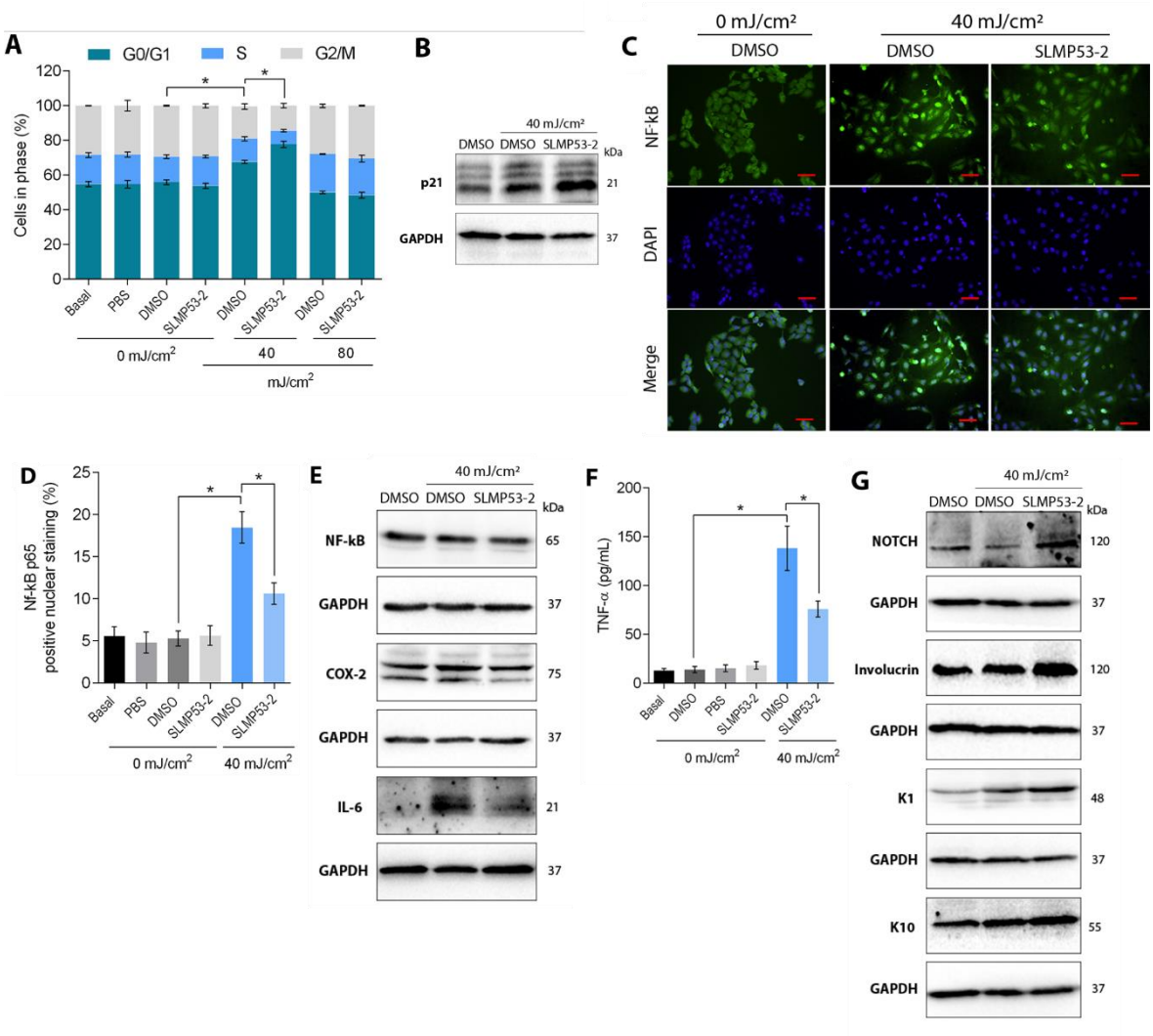


Figure 14 – SLMP53-2 induces cell cycle arrest and differentiation and suppresses inflammation in UVB-irradiated keratinocyte cells.

(A) Effect of 3.5 µM SLMP53-2 pre-treatment on cell cycle progression of HaCaT cells 20h after 40 or 80 mJ/cm^2 UVB irradiation. Cell cycle phases were analysed by flow cytometry using PI staining and quantified using the FlowJo software. Data are mean ± SEM of 4 independent experiments; values significantly different from non-irradiated DMSO (control) and from irradiated DMSO-treated cells: *p < 0.05 (One-Way ANOVA Tukey's multiple comparisons test). **(B)** Protein levels of p21 in HaCaT cells pre-treated with 3.5 µM SLMP53-2 for 24h followed by 40 mJ/cm^2 UVB radiation. Protein levels were analysed for 20h after irradiation by western blot. Immunoblots are representative of 3 independent experiments; GAPDH was used as loading control. **(C-D)** SLMP53-2 effect on NF-kB (p65 subunit) nuclear translocation in HaCaT cells pre-treated with 3.5 µM SLMP53-2 for 24h and followed by 40 mJ/cm^2 UVB radiation. Assay performed for 6h after UVB exposure. Representative images of 4 independent experiments; scale bar = 50 µm; magnification = ×200. Data are mean ± SEM of 4 independent experiments; values significantly different from non-irradiated DMSO (control) and from irradiated DMSO-treated cells: *p < 0.05 (One-Way ANOVA Tukey's multiple comparisons test). **(E)** Protein levels of inflammatory markers in HaCaT cells pre-treated with 3.5 µM SLMP53-2 for 24h followed by 40 mJ/cm^2 UVB radiation. Protein levels were analysed 20h after irradiation (6h for NF-kB, p65 subunit) by western blot. Immunoblots are representative of 3 independent experiments; GAPDH was used as a loading control. **(F)** Determination of TNF-α secreted levels in HaCaT pre-treated with 3.5 µM SLMP53-2 for 24h and followed by 40 mJ/cm^2 UVB radiation. TNF-α secreted levels were analysed 20h after irradiation by ELISA. Data are mean ± SEM of 5 independent experiments; values significantly different from non-irradiated DMSO (control) and from irradiated DMSO-treated cells: *p < 0.05 (One-Way ANOVA Tukey's multiple comparisons test). **(G)** Protein levels of differentiation markers in HaCaT cells pre-treated with 3.5 µM SLMP53-2 for 24h and followed by 40 mJ/cm^2 UVB radiation. Protein levels

were analysed for 20h after irradiation by western blot. Immunoblots are representative of 3 independent experiments; GAPDH was used as a loading control.

3. SLMP53-2 Protects Against UVB-induced Cell Death with Inhibition of Oxidative Damage

The effect of the SLMP53-2 pre-treatment in cell death and oxidative stress in UVB-irradiated keratinocyte cells was also assessed. The obtained results showed that 80mJ/cm^2 UVB radiation significantly induced apoptosis in HaCaT cells (Figure 15A), associated with increased levels of phosphorylated JNK (p-JNK), cleaved PARP and caspase-3 protein levels (Figure 15B). Notably, 3.5 μM SLMP53-2 pre-treatment was able to inhibit all these effects (Figure 15A, B).

We further verified a marked induction of ROS generation in 80mJ/cm^2 UVB-irradiated keratinocyte cells, when compared to non-irradiated cells, which was also counteracted by 3.5 μM SLMP53-2 pre-treatment (Figure 15C). Consistently, significant modifications in proteins and lipids caused by ROS and RNS, particularly lipid peroxidation (measured by the 4-hydroxynonenal levels), protein nitrosylation (measured by the 3-nitrotyrosine levels), and protein carbonylation (measured by the dinitrophenyl levels, were markedly promoted by 80mJ/cm^2 UVB radiation and significantly reduced by 3.5 μM SLMP53-2 pre-treatment (Figure 15D).

Altogether, these results showed a protective effect of SLMP53-2 against UVB-induced apoptotic cell death and oxidative damages.

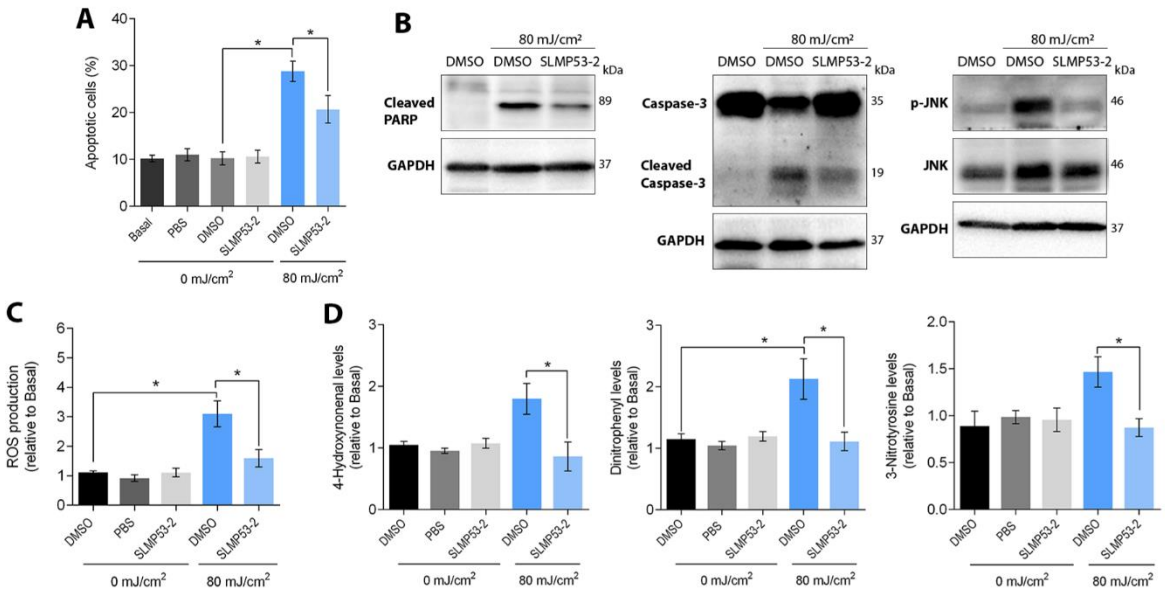


Figure 15 – SLMP53-2 protects against apoptotic cell death, inhibiting oxidative damage in UVB-irradiated keratinocyte cells.

(A) Effect of 3.5 μM SLMP53-2 pre-treatment on apoptosis induction in HaCaT cells, 10h after 80 mJ/cm^2 UVB irradiation. Percentage of Annexin-positive cells was analysed by flow cytometry using PI and Annexin-V staining and quantified using the FlowJo software. Data are mean ± SEM of 5 independent experiments; values significantly different from non-irradiated DMSO (control) and from irradiated DMSO treated cells: *p < 0.05 (One-Way ANOVA Tukey's multiple comparisons test). **(B)** Protein levels of cleaved PARP, caspase-3 and p-JNK in HaCaT cells pre-treated with 3.5 μM SLMP53-2 for 24h followed by 80 mJ/cm^2 UVB radiation. Protein levels were analysed for 6h (p-JNK) or 20h (Caspase-3 and PARP) after irradiation by western blot. Immunoblots are representative of 3 independent experiments; GAPDH was used as a loading control. **(C)** ROS generation was measured through DCF fluorescence in HACAT cells pre-treated with 3.5 μM SLMP53-2 for 24h followed by 80 mJ/cm^2 UVB radiation. Measurement of ROS production was performed 20h after irradiation. Results are plotted in percentage of basal DMSO-treated cells and are mean ± SEM of 4 independent experiments. Values significantly different from non-irradiated DMSO (control) and from irradiated DMSO-treated cells: *p < 0.05 (One-Way ANOVA Tukey's multiple comparisons test). **(D)** Oxidative damage measured by evaluation of lipid peroxidation and of proteins carbonylation and nitration, respectively, through slot-blot method, 6h after irradiation. Results are plotted in percentage of basal DMSO-treated cells and data are mean ± SEM of 4-8 independent experiments. Values significantly different from non-irradiated DMSO (control) and from the respective irradiated DMSO-treated cells: *p < 0.05 (One-Way ANOVA Tukey's multiple comparisons test).

4. SLMP53-2 depletes UVB-induced DNA-damage

Considering the effect of SLMP53-2 on the promotion of cell survival for 80 mJ/cm^2, we aimed to ascertain the impact of this compound in the DNA damage repair pathway. For that, a T4 endonuclease-modified alkaline comet assay (Figure 16A) and an immunofluorescence analysis of the phosphorylation of histone H2AX on serine 139 (γH2AX) (Figure 16B) were performed. The first assay enables to evaluate specific UVB-induced DNA damages, since the T4 endonuclease specifically cleaves pyrimidine dimers [83]. In 80mJ/cm^2 UVB-irradiated cells, we detected an increase in type BCD and E nucleoids (containing completely damaged DNA [84]) and a decrease in type A nucleoids (containing undamaged DNA [84]), compared to the non-irradiated control (Figure 16A). Accordingly, in 3.5 μM SLMP53-2 pre-treated cells, an increase in the number of type A nucleoids and a decrease in the number of type BCD and E nucleoids were observed, indicating a protective effect of SLMP53 on UVB-induced DNA damage. In addition, 80mJ/cm^2 UVB radiation increased comet tail length, percentage of DNA in the tail and tail moment (Figure 16A, B), and interfered with the levels of γH2AX (a common marker of DSBs [85]), enhancing the percentage of cells with >10 foci, while decreasing the percentage of cells with 0-5 foci (Figure 16C, D). Notably, these parameters were also significantly reverted upon 3.5 μM SLMP53-2 pre-treatment.

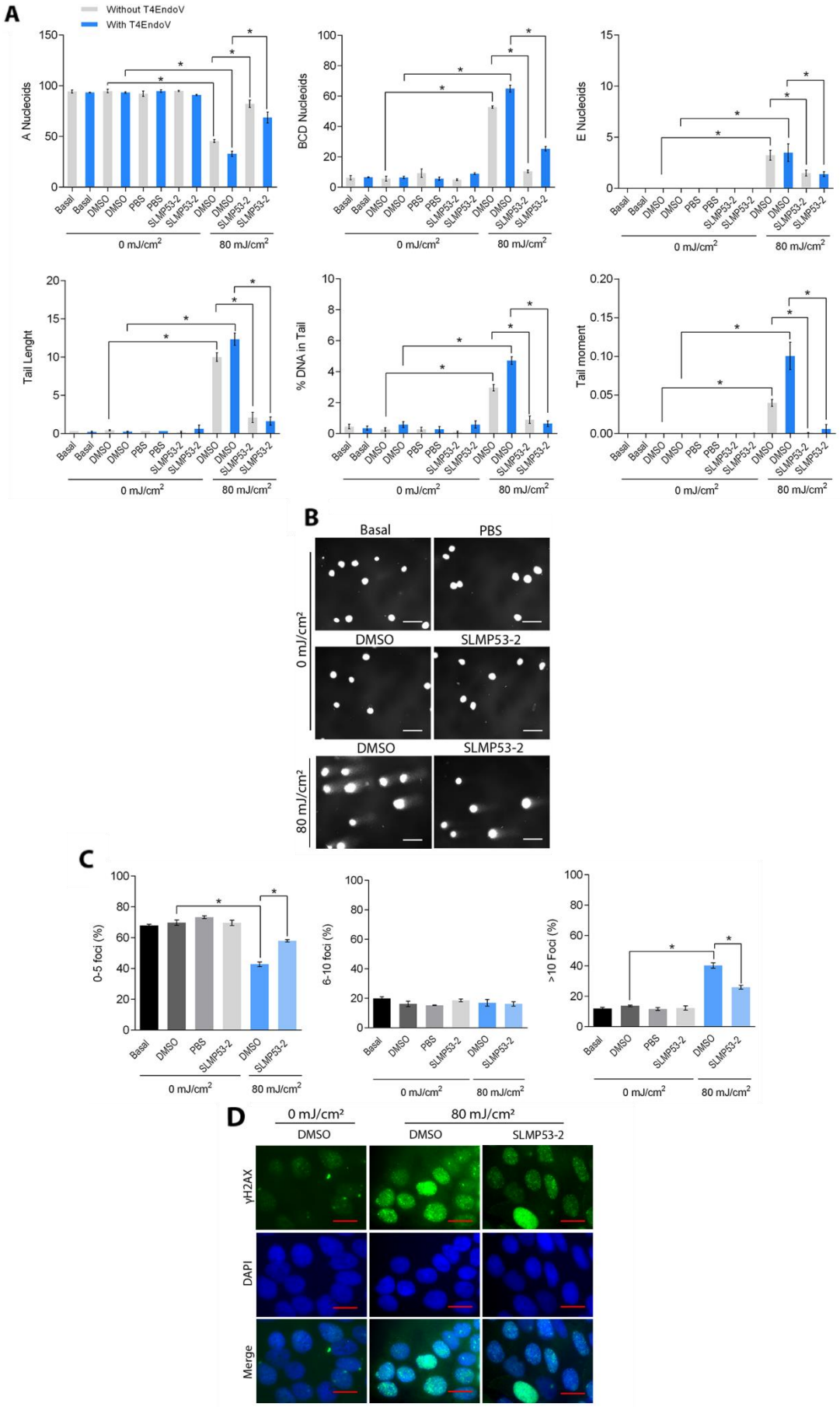


Figure 16 – SLMP53-2 reduces DNA damage in UVB-irradiated keratinocyte cells.

(A, B) Protective effect of 24h pre-treatment with 3.5 μM SLMP53-2 on 80 mJ/cm^2 UVB-induced DNA damage. Genotoxicity was assessed by T4 endonuclease-modified alkaline comet assay immediately after UVB-irradiation. In A, DNA damage is reported as percentage of nucleoids type (A, BCD, and E), tail length, percentage of DNA in the tail (% DNA in Tail) and tail moment. Results are mean ± SEM of 3 independent experiments. Values significantly different from non-irradiated DMSO: **p* < 0.05 (One-Way ANOVA test, Dunnett's multiple comparison test), and from the corresponding irradiated DMSO-treated cells **p* < 0.05 (Two-Way ANOVA test, Bonferroni post-test); In B, representative images from T4 endonuclease-modified alkaline comet assay, of 3 independent experiments; scale bar = 10 μm; magnification = ×400. **(C, D)** Protective effect of 3.5 μM SLMP53-2 24h pre-treatment on 80 mJ/cm^2 UVB-induced DSBs formation. The presence of DSBs was evaluated with immunostaining of γH2AX histone 1h after irradiation. In C, data are presented as percentage of cells with 0–5, 6–10 and more than 10 foci (%) and are means ± SEM of 3 independent experiments. Values significantly different from non-irradiated DMSO (control): **p* < 0.05 (One-Way ANOVA test, Dunnett's multiple comparison test), and from the corresponding DMSO treated cells irradiated **p* < 0.05 (Two-Way ANOVA test, Bonferroni post-test); In D, representative images of 3 independent experiments; scale bar = 5 μm; magnification = ×1000.

For an in-depth analysis of the effect of SLMP53-2 on UVB-induced DNA damage, the levels of CPDs formation were investigated by immunofluorescence assay, after 6 h of UVB exposure (since at this time point, the repair pathways achieve the highest activity). As expected, 80mJ/cm^2 UVB radiation enhanced the percentage of CPD positive cells and the intensity of the fluorescence signal (mean fluorescence) (Figure 17A, B). Once again, the pre-treatment with SLMP53-2 decreased the extent of this type of DNA damage (Figure 17A, B).

Subsequently, considering the role of p53 in DNA repair, particularly in the NER pathway, the effect of SLMP53-2 in this cellular process was investigated. For that, we checked the protein expression levels of XPC and DDB-2, for 1 - 6h after UVB exposure, by immunofluorescence and western blot analysis (Figure 17C-G). In the immunofluorescence assay, although the exposure of keratinocyte cells to 80mJ/cm^2 UVB radiation did not interfere with the expression levels of these two p53 targets, the SLMP53-2 pre-treatment significantly increased their expression levels in 80mJ/cm^2 UVB-irradiated cells, when compared to DMSO (Figure 17C-F). Of note, although not significant, a visible increase of XPC and DDB-2 levels could already be observed in non-irradiated cells pre-treated with SLMP53-2, when compared to DMSO, in immunofluorescence assay (Figure 17C, E). These results were further supported by western blot analysis, which further evidenced an increase of the XPC and DDB-2 levels by SLMP53-2 pre-treatment. Interestingly, by western blot analysis, we could also observe a decrease of the XPC and DDB-2 expression levels triggered by 80mJ/cm^2 UVB radiation after 6h exposure (Figure 17G), which support the stimulation of a degradation pathway for these protein by UVB radiation [86, 87].

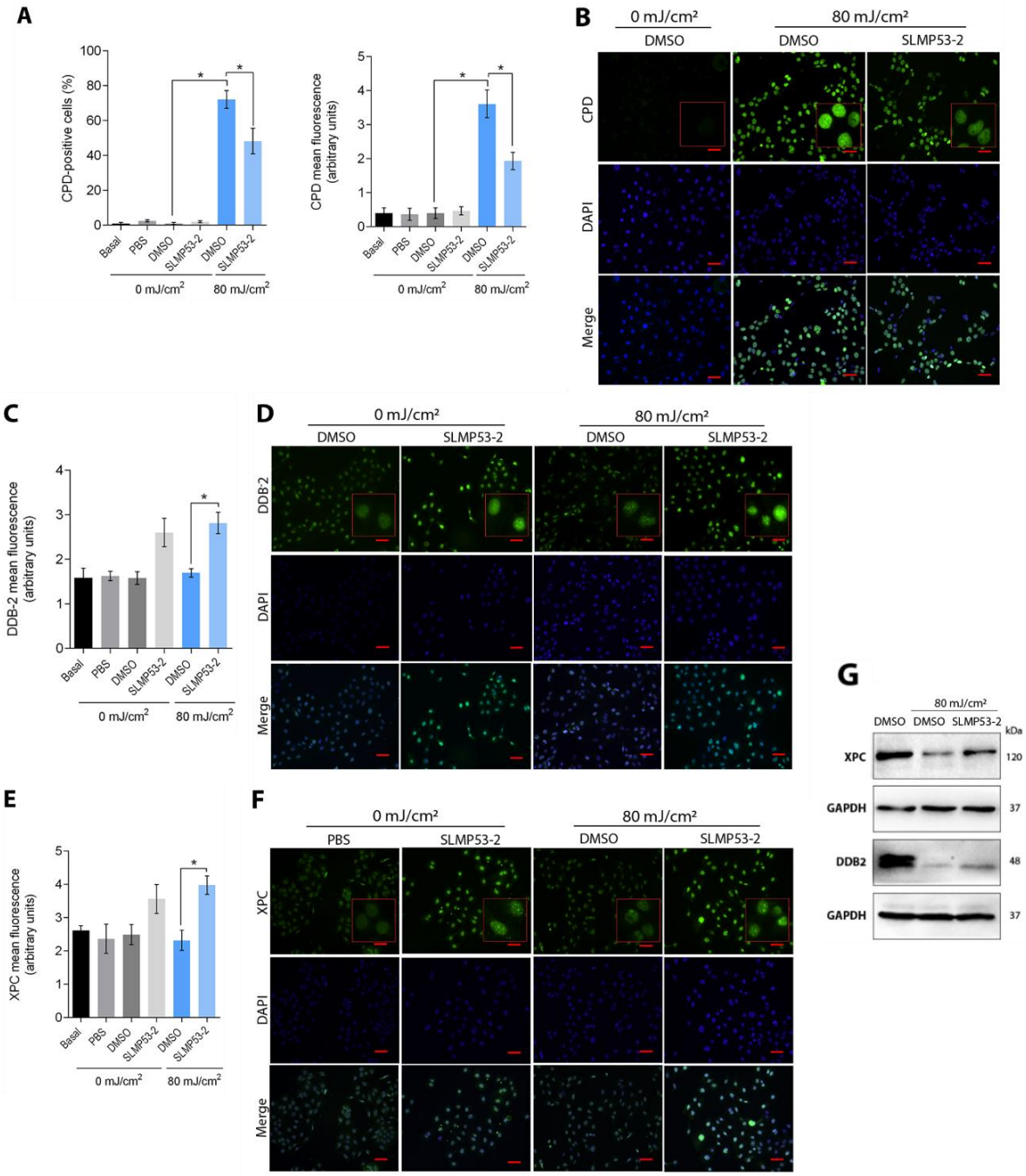


Figure 17 - SLMP53-2 protects against UVB-induced CPD and increases the levels of the NER-related proteins XPC and DDB-2.

(A, B) Protective effect of 3.5 µM SLMP53-2 24h pre-treatment on 80 mJ/cm^2 UVB-induced CPDs. The immunofluorescence analysis was performed 6h after the irradiation of the cells. In **A**, data are presented as percentage of positive cells stained with CPD antibody and as mean of fluorescence. Data are means ± SEM of 5 independent experiments. Values significantly different from non-irradiated DMSO (control) and from irradiated DMSO-treated cells: *p < 0.05 (One-Way ANOVA Tukey's multiple comparisons test). In **B**, representative images of 5 independent experiments; scale bar = 50 µm; magnification = ×200. **(C-F)** DNA-repair enhancement by 3.5 µM SLMP53-2 24h pre-treatment on 80 mJ/cm^2 UVB exposed cells. The evaluation of the DDB-2 and XPC fluorescence staining was performed 1h after the irradiation of the cells by immunofluorescence analysis. In **C**, data are presented as mean fluorescence of DDB-2. Data are means ± SEM of 3 independent experiments. Values are not significantly different from non-irradiated DMSO (control) and from irradiated DMSO-treated cells: *p > 0.05 (One-Way ANOVA Tukey's multiple comparisons test). In **D**, representative images of 3 independent experiments; scale bar = 50 µm; magnification = ×200. In **E**, data are presented as mean fluorescence of XPC. Data are

means ± SEM of 3 independent experiments. Values are not significantly different from non-irradiated DMSO (control) and from irradiated DMSO-treated cells: *p > 0.05 (One-Way ANOVA Tukey's multiple comparisons test). In **F**, representative images of 3 independent experiments; scale bar = 50 µm; magnification = ×200. **(G)** Protein levels of major NER pathway proteins in HaCaT cells pre-treated with 3.5 µM SLMP53-2 for 24h and then exposed to 80 mJ/cm^2 UVB radiation. Protein levels were analysed for 6h after irradiation by western blot. Immunoblots are representative of 3 independent experiments; GAPDH was used as a loading control.

Altogether, these results indicated that SLMP53-2 protected keratinocyte cells against DNA damage, specifically by inhibiting UVB-induced CPDs and increasing the protein levels of relevant players of the NER pathway of the DNA damage repair.

5. *In vivo* protective effect of SLMP53-2

To evaluate the *in vivo* protective activity of SLMP53-2, 1.5 mg SLMP53-2 was topically applied in FVB/N mice for 1 hour prior to 180 mJ/cm^2 UVB irradiation. The mice skin tissues were collected 24 hours after UVB exposure for immunofluorescence and immunohistochemistry analysis.

By immunofluorescence analysis of CPDs levels, we also confirmed *in vivo* an induction of CPDs formation in the epidermis of UVB irradiated mice, which was markedly reduced in SLMP53-2 pre-treated mice (Figure 18A). We also studied the impact of SLMP53-2 on the modulation of the DNA repair pathway in vivo by analysis of the XPC and DDB-2 expression levels, in mice skin (Figure 18B). The UVB radiation markedly decreased the DDB-2 expression levels, while it did not significantly interfere with the XPC levels. However, as observed *in vitro*, a marked reversion of UVB effect could be observed in SLMP53-2 pre-treated mice (Figure 18B). These results reinforced the enhancement of the NER pathway by SLMP53-2 as a mechanism of DNA repair in UVB-irradiated mice.

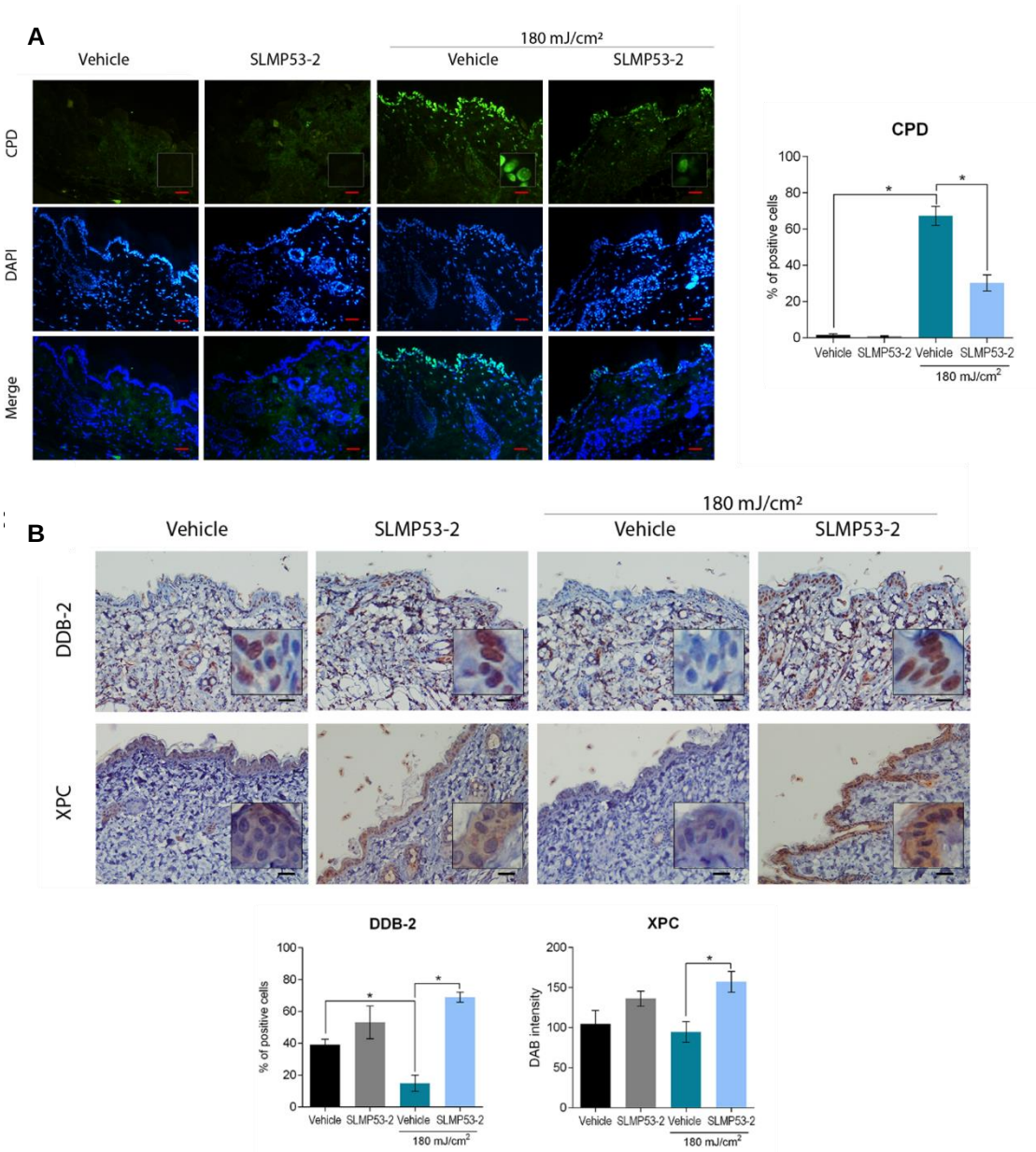


Figure 18 - SLMP53-2 inhibits CPD formation and stimulates NER DNA repair pathway in mice skin.

(A, B) Evaluation of CPD formation by immunofluorescence **(A)** or protein levels by DAB staining **(B)** was performed in skin tissues collected 24h after UVB irradiation (180 mJ/cm^2) of the animals. In A, scale bar = 50 μm; magnification = 200×. In B, scale bar = 10 μm; magnification = 200×. Images are representative of 5 independent experiments. Quantification of CPD positive cells and of DAB intensity for DDB-2 and XPC. Data are means ± SEM of 5 independent experiments. Values significantly different from non-irradiated control animals (*p < 0.05) and from vehicle-treated irradiated animals (*p < 0.05; One-Way ANOVA Tukey's multiple comparisons test).

Considering the effect of UVB radiation in the induction of apoptosis, the TUNEL assay (for the measurement of DNA fragmentation [88]) was performed (Figure 19). the measurement of DNA fragmentation [88]. As *in vitro*, we observed a significant induction of apoptosis by UVB radiation, which was reverted upon pre-treatment with SLMP53-2 in mice

skin. This result highlights that SLMP53-2 not only protects against DNA damage, through enhancement of DNA repair, but also from programmed cell death.

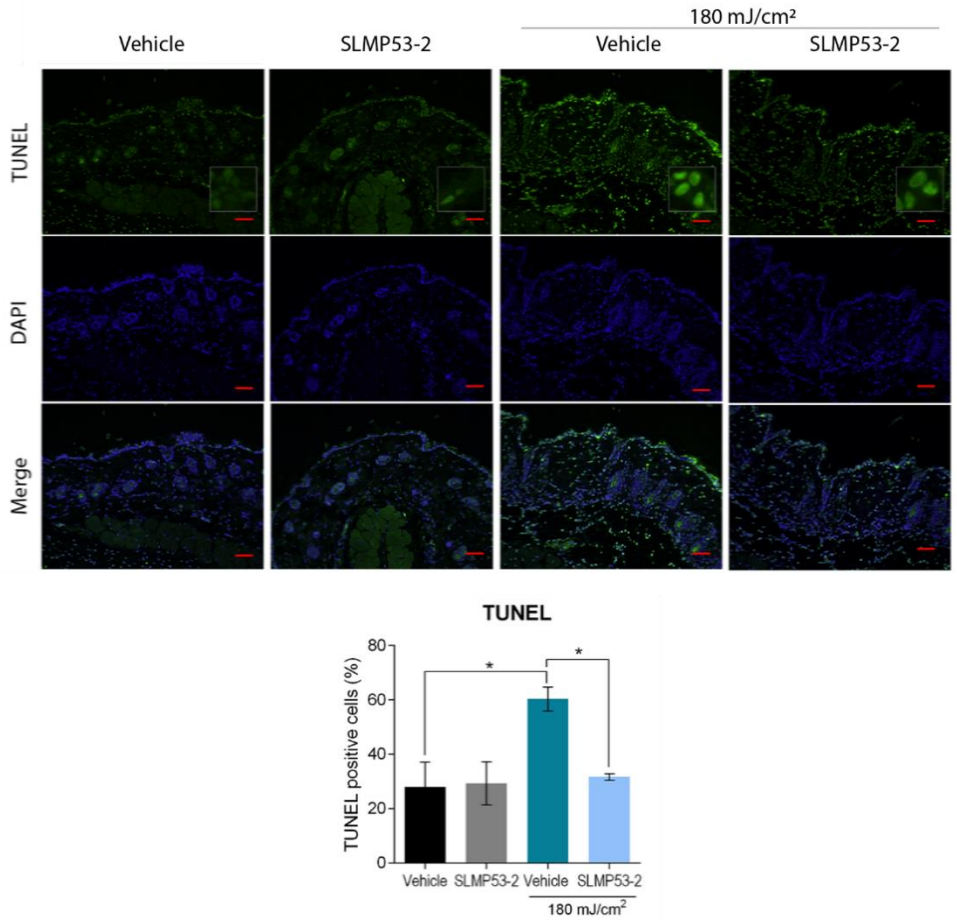


Figure 19 – SLMP53-2 inhibits apoptosis in mice skin.
TUNEL assay by immunofluorescence was performed in skin tissues collected 24h after UVB irradiation (180 mJ/cm^2) of the animals. Quantification of TUNEL positive cells. Values significantly different from non-irradiated control animals (*$p < 0.05$) and from vehicle-treated irradiated animals (*$p < 0.05$; One-Way ANOVA Tukey's multiple comparisons test). Scale bar = 50 μm; magnification = 200×. Images are representative of 5 independent experiments.

The effect of SLMP53-2 on inflammation and differentiation was also explored *in vivo.* Regarding inflammation, the levels of the inflammatory mediators, COX-2 and IL-6, were evaluated by immunofluorescence staining of skin tissues (Figure 20A). The results revealed a stimulation of the expression levels of these markers by UVB radiation, which was reverted by SLMP53-2 pre-treatment in UVB-irradiated mice. The levels of the differentiation markers, K1 and involucrin, were also analysed by immunohistochemistry analysis (Figure 20B). In agreement with the obtained *in vitro*, SLMP53-2 enhanced the expression levels of K1 and involucrin in UV-irradiated skin.

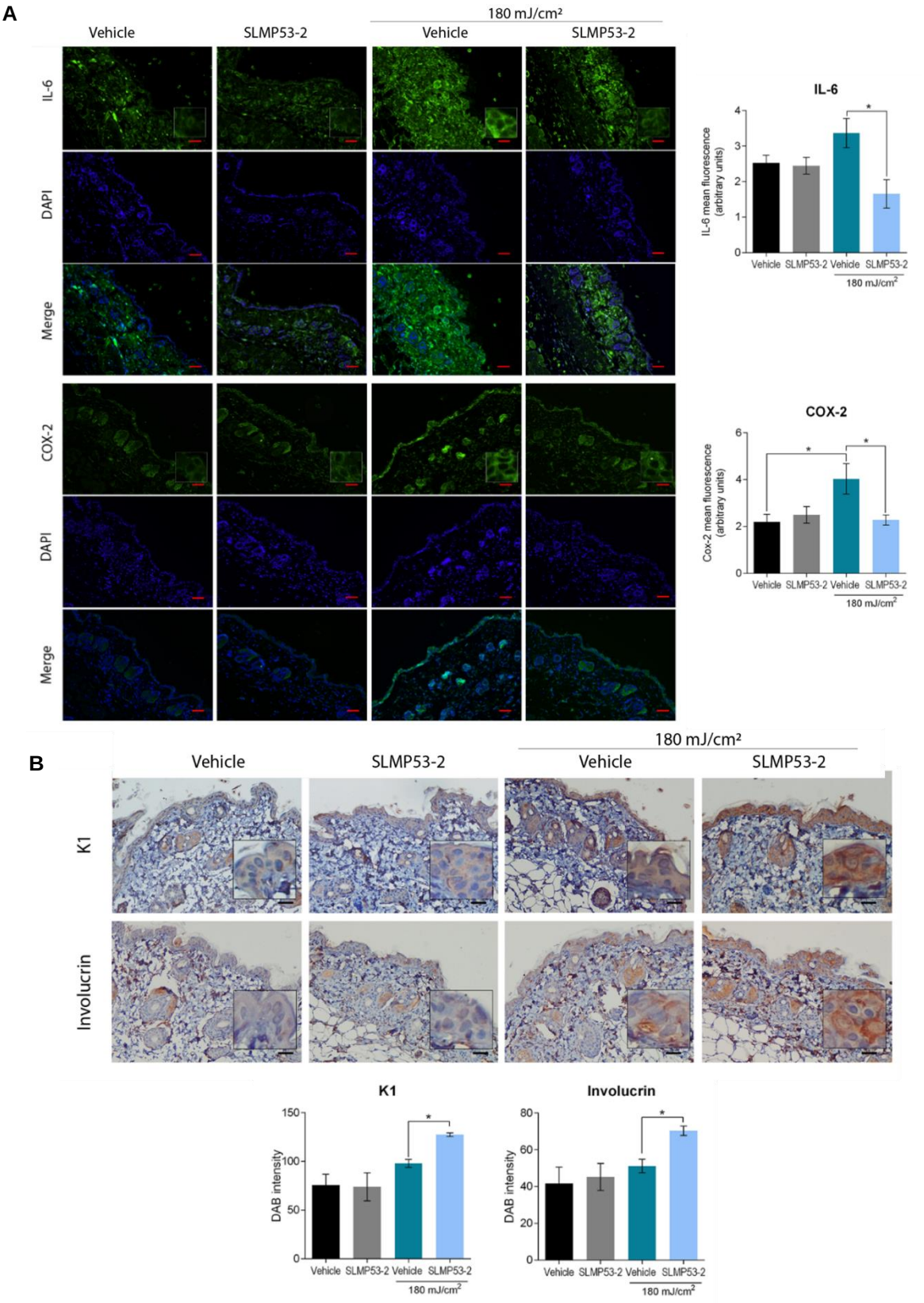


Figure 20 - SLMP53-2 inhibits inflammation and promotes differentiation in skin mice.

(A, B) Evaluation of different protein expression levels by immunofluorescence (A) or DAB staining (B) were performed in skin tissues collected 24h after the irradiation (180 mJ/cm^2) of the animals. In A, scale bar = 50 μm; magnification = 200×. In B, scale bar = 10 μm; magnification = 200×). Images are representative of 5 independent experiments. Quantification of mean fluorescence for COX-2 and IL-6 and of DAB intensity for K1 and Involucrin. Data are means ± SEM of 5 independent

experiments. Values significantly different from non-irradiated control animals (*$p < 0.05$) and from vehicle-treated irradiated animals (*$p < 0.05$; One-Way ANOVA Tukey's multiple comparisons test).

Chapter IV: Discussion and Conclusion

The rising incidence rates have encouraged the search and development of chemopreventive agents against SC formation and progression. Since UVR injurious effects are major contributors for skin carcinogenesis, preventing their occurrence represents a valuable approach for avoiding skin cancer [58]. In fact, several natural and synthetic compounds have already shown promising results in preventing UVR-induced skin cancer through the elimination of DNA damage, inflammation, and oxidative stress [67-70].

The *TP53* gene regularly presents UV-signature mutations in UVR-induced NMSC [58]. As a result, its tumor suppressor function is compromised. Most importantly, the mutp53 that are formed contribute to malignant transformation [28]. In conformity with several studies [71-73], the reactivation of p53 constitutes a promising strategy of UV-induced SC prevention. SLMP53-2, a small molecule identified by our group in previous work [75], is a mutp53 reactivator that exerts its function through the reestablishment of the wt-like conformation to mutp53, consequently restoring its wt function. As such, in the present thesis, we studied the potential of SLMP53-2 as a SC chemopreventive agent.

The HaCaT cell line expresses two point mutations in *TP53* at dypirimidine sites, R282Q and H179Y, characteristic of UVR-induced mutations, that lead to LOF [89]. Also, GOF of these mutants was described in this cell line [89]. We showed that SLMP53-2 treatment of HaCaT cells reduced the levels of mutp53, supporting the reactivation of mutp53 through the acquisition of a wt-like conformation, as previously demonstrated [75]. In fact, SLMP53-2 treatment, before UVB exposure, resulted in the upregulation of several p53 target genes, including p21 (a cell cycle regulator), XPC and DDB-2 (DNA repair proteins) and NOTCH-1 (differentiation regulator), which further supported that the compound was able to restore the transcriptional activity of mutp53.

We also observed an increase in the survival of UVB-irradiated cells upon pre-treatment, which can be associated with the ability of p53 to inhibit UVR-induced damage. In fact, our results showed that HaCaT cells undergo cell cycle arrest in G1-phase upon 40 mJ/cm^2 UVB exposure, which was further enhanced by SLMP53-2 pre-treatment. This result is in accordance with an increase in p21 protein levels for this UVB dose that was promoted in the SLMP53-2 pre-treated cells. Importantly, p21 is known to also have a role in DNA repair and in blocking apoptosis induced by DNA damage. Thus, the increase of p21 in the SLMP53-2-treated cells correlates with the increase in cell survival of irradiated cells, potentially favoring a reduction in UVB-induced cell death [90].

UVR causes severe damage in irradiated cells and leads to the activation of cell signaling pathways, namely the MAPK, that lead to the induction of apoptosis. In fact, we observed a great induction of apoptosis upon 80 mJ/cm^2 UVB exposure. Moreover, for this

UVB radiation, SLMP53-2 protected keratinocytes from UVR-induced apoptosis, which is associated with a decrease in caspase-3 and PARP cleavage. In fact, PARP is cleaved/inactivated by activated caspase 3 in the execution pathway of apoptosis, which increases apoptotic DNA fragmentation [91]. Regarding the phosphorylation of JNK (a MAPK), studies have shown that this event is necessary for UV-induced apoptosis [92]. When active, JNK eventually leads to the activation of AP-1, which upregulates the expression of pro-apoptotic factors [92]. Interestingly, SLMP53-2 also decreased the phosphorylation of JNK, supporting the decrease in UVB-induced apoptosis.

Additionally, SLMP53-2 reduced ROS levels in UVB-irradiated cells for 80 mJ/cm^2. In fact, the p53 antioxidant activity has been extensively described, being highly dependent on the cellular context [93]. Upon oxidative stress, p53 protects cells from oxidative damage by inducing the expression of target genes involved in antioxidation, such as glutathione peroxidase (GPX) and aldehyde dehydrogenase (ALDH) [93]. This antioxidant function of p53 justifies the reduction of the ROS levels, in SLMP53-2 treated cells. The inhibition of the oxidative state of the irradiated cells by SLMP53-2 treatment is evidenced by the decrease in the lipid peroxidation, protein nitrosylation and protein carbonylation, protecting cells against oxidative damage. ROS also positively regulates JNK activity by inhibiting JNK phosphatases, among other mechanisms [94]. This exposes another mechanism for reduction of JNK phosphorylation. Finally, considering the role of ROS in inducing apoptosis, the reduction of the ROS levels is consistent with a decrease in the percentage of apoptotic cells.

We also analyzed the effect of SLMP53-2 on UVB-induced DNA damage, namely in the formation of CPDs and DSBs. The assessment of DNA damage is a crucial part of the work, considering the importance of UVB-induced DNA damage in mutagenesis and, consequently, carcinogenesis. Moreover, DNA repair is one of the main functions of p53 in protecting cells against tumorigenesis. Notably, SLMP53-2 greatly reverted the occurrence of UVB-induced DNA damage, which was induced by 80mJ/cm^2 of UVB radiation. Then, we studied the mechanism by which SLMP53-2 could protect keratinocytes against DNA damage. The CPDs produced by UVB radiation cause bulky lesions, which are mainly repaired by the NER pathway [54]. As such, we analyzed the effect of SLMP53-2 in NER pathway proteins. SLMP53-2 induced the expression of XPC and DDB-2 in UVB-irradiated cells, which participate in the recognition of damage in this pathway, establishing a crossing point between p53 and the repair of UVR-induced DNA damage. Of note, we observed that SLMP53-2 induced their expression previously to the stimuli. It is already described that upon DNA damage, the expression of NER pathway proteins is promoted following by proteasomal degradation [86, 87]. In fact, we noticed that 6 hours after UVB exposure, the

levels of XPC and DDB-2 were slightly decreased, which confirmed the degradation of these proteins over the time. Notably, SLMP53-2 counteracted the observed degradation of these NER proteins, stimulating its transcription and, consequently, the DNA repair. These results revealed that SLMP53-2 reduced DNA damage through the induction of NER pathway proteins and by a p53-dependent manner. Altogether, the protection of irradiated cells from death by SLMP53-2 arises from the induction of cell cycle arrest, antioxidant activity, and DNA repair.

Inflammation, a hallmark of cancer, is an important effect of UVR on skin. NF-κB is a central component in the inflammatory response directly activated by UVR. When active, it leads to the production of pro-inflammatory mediators, such as IL-6, TNF-α and COX-2. TNF-α, in turn, binds to TNF receptors (TNFR), promoting NF-κB activation and the activation of other signaling pathways such as p38 MAPK and JNK. In fact, we observed that 40 mJ/cm^2 UVB exposure increase NF-κB, IL-6 and COX-2 levels, and the secretion of TNF-α. On the other hand, it is already well described that p53 is a negative regulator of inflammation, which is mediated by its antagonistic relationship with NF-κB. In particularly, studies in human colon cancer cells showed that p53 blocks the translocation of NF-κB from the cytoplasm to the nucleus, inhibiting its activity [95]. In this study, even though SLMP53-2 pre-treatment did not reduce the levels of NF-κB in UVB-irradiated cells, we observed a decrease in the nuclear translocation of this transcriptional factor, which is essential for its transcriptional activity. Also, we observed a decrease in COX-2 and IL-6 expression, and a decrease in TNF-α secretion in SLMP53-2 treated cells, which is associated with a decrease in NF-κB activity. Moreover, ROS mediates inflammation through the activation of the transcriptional factors NF-KB and AP-1 [96]. So, the reduction of ROS levels with SLMP53-2 treatment is also associated with a decline in inflammation.

The effect of SLMP53-2 on differentiation was also analyzed in UVB-exposed cells. UVR induces keratinocyte differentiation, which may function as a protective mechanism against the accumulation of damaged cells and, consequently, carcinogenesis [68, 97]. Consistently, in the SLMP53-2 pre-treated cells, we observed an enhancement of the differentiation of irradiated keratinocytes with an increase of the levels of the differentiation markers K1, K10, involucrin and NOTCH-1 upon 40 mJ/cm^2 of UVB radiation. Even though UVR induced differentiation, the NOTCH-1 levels appear decreased. Since HaCaT cells express mutp53, we hypothesized that it could not lead to the upregulation of NOTCH-1. So, the differentiation observed in keratinocytes possibly occurs through a NOTCH-1-independent manner.

The activity of SLMP53-2 in the protection against UVB-induced damage was also evaluated *in vivo*. As expected, UVB radiation led to DNA damage mediated by the

formation of CPDs, which was inhibited by SLMP53-2. Furthermore, in UVB-irradiated mice, the promotion of the DNA repair by SLMP53-2 was mediated by the enhancement of the expression of the NER pathway proteins. Consistently, the reduction of apoptosis by SLMP53-2 was also observed *in vivo*. Finally, the effect of SLMP53-2 on inflammation and differentiation observed in *in vitro* analysis was further supported in UVB-irradiated mice.

In conclusion, the results herein obtained support that SLMP53-2 has promising activity in the protection against UVR-induced skin carcinogenesis. SLMP53-2 reveals therefore great potential to be used in SC chemoprevention, which by definition comprises the use of non-cytotoxic drugs to halt malignant transformation [98]. Since carcinogenesis is a slow multi-step process, targeting a specific regulator from those steps reveals to be a promising strategy against carcinogenesis [99]. SLMP53-2 specifically targets mutp53, which could prevent non-desirable secondary effects of UVR. The use of chemopreventive agents such as SLMP53-2 would be relevant in high-risk populations, such as people with fair skinned or skin cancer history, who are at high risk of developing second primary tumors [99].

In the near future, the SLMP53-2 could be used as a topical cream formulation before sun exposure. Also, the compound could be formulated in synergy with sunscreen for a greater protection against UVR.

References

[1] WHO. (2020, 20 May). *Cancer* [Online]. Available: https://www.who.int/news-room/fact-sheets/detail/cancer.

[2] H. Sung *et al.*, "Global Cancer Statistics 2020: GLOBOCAN Estimates of Incidence and Mortality Worldwide for 36 Cancers in 185 Countries," (in eng), *CA Cancer J Clin,* vol. 71, no. 3, pp. 209-249, May 2021.

[3] R. Gordon, "Skin Cancer: An Overview of Epidemiology and Risk Factors," *Seminars in oncology nursing,* vol. 29, no. 3, pp. 160 - 169, 2013.

[4] E. M. Ferlay J, Lam F, Colombet M, Mery L, Piñeros M, Znaor A, Soerjomataram I, Bray F (2020, 20 May). *Global Cancer Observatory: Cancer Today* [Online]. Available: https://gco.iarc.fr/today.

[5] H. R. Keller, X. Zhang, L. Li, H. Schaider, and J. W. Wells, "Overcoming resistance to targeted therapy with immunotherapy and combination therapy for metastatic melanoma," (in eng), *Oncotarget,* vol. 8, no. 43, pp. 75675-75686, Sep 26 2017.

[6] D. Didona, G. Paolino, U. Bottoni, and C. Cantisani, "Non Melanoma Skin Cancer Pathogenesis Overview," (in eng), *Biomedicines,* vol. 6, no. 1, Jan 2 2018.

[7] V. Madan, J. T. Lear, and R.-M. Szeimies, "Non-melanoma skin cancer," *The Lancet,* vol. 375, no. 9715, pp. 673-685, 2010.

[8] H. Yousef, M. Alhajj, and S. Sharma, *Anatomy, Skin (Integument), Epidermis*. StatPearls Publishing, Treasure Island (FL), 2020.

[9] E. Ogawa *et al.*, "p63/p51-induced onset of keratinocyte differentiation via the c-Jun N-terminal kinase pathway is counteracted by keratinocyte growth factor," (in eng), *J Biol Chem,* vol. 283, no. 49, pp. 34241-34249, 2008.

[10] E. Candi, R. Schmidt, and G. Melino, "The cornified envelope: a model of cell death in the skin," *Nature Reviews Molecular Cell Biology,* vol. 6, no. 4, pp. 328-340, 2005/04/01 2005.

[11] S. Shetty and S. Gokul, "Keratinization and its disorders," (in eng), *Oman Med J,* vol. 27, no. 5, pp. 348-357, 2012.

[12] R. Gordon, "Skin cancer: an overview of epidemiology and risk factors," (in eng), *Seminars in oncology nursing,* vol. 29, no. 3, pp. 160-9, Aug 2013.

[13] N. Boulais and L. Misery, "Merkel cells," *Journal of the American Academy of Dermatology,* vol. 57, no. 1, pp. 147-165, 2007/07/01/ 2007.

[14] D. Didona, G. Paolino, U. Bottoni, and C. Cantisani, "Non Melanoma Skin Cancer Pathogenesis Overview," *Biomedicines,* vol. 6, no. 1, p. 6, 2018.

[15] J. Schmitt, A. Seidler, T. L. Diepgen, and A. Bauer, "Occupational ultraviolet light exposure increases the risk for the development of cutaneous squamous cell carcinoma: a systematic review and meta-analysis," (in eng), *The British journal of dermatology,* vol. 164, no. 2, pp. 291-307, Feb 2011.

[16] J. A. Siegel, K. Korgavkar, and M. A. Weinstock, "Current perspective on actinic keratosis: a review," (in eng), *The British journal of dermatology,* vol. 177, no. 2, pp. 350-358, Aug 2017.

[17] B. Daniel and C. O. Clark, "Skin cancer in organ transplant recipients: Epidemiology, pathogenesis, and management," *Journal of the American Academy of Dermatology,* vol. 47, no. 1, pp. 1-20, 2002.

[18] R. Abeti *et al.*, "Xeroderma pigmentosum: overview of pharmacology and novel therapeutic strategies for neurological symptoms," (in eng), *Br J Pharmacol,* vol. 176, no. 22, pp. 4293-4301, Nov 2019.

[19] D. Schadendorf *et al.*, "Melanoma," *The Lancet,* vol. 392, no. 10151, pp. 971-984, 2018.

[20] J. Read, K. A. W. Wadt, and N. K. Hayward, "Melanoma genetics," *Journal of Medical Genetics,* vol. 53, no. 1, pp. 1-14, 2016.

[21] D. L. Narayanan, R. N. Saladi, and J. L. Fox, "Review: Ultraviolet radiation and skin cancer," *International Journal of Dermatology,* vol. 49, no. 9, pp. 978-986, 2010.

[22] C. SEEBODE, J. LEHMANN, and S. EMMERT, "Photocarcinogenesis and Skin Cancer Prevention Strategies," *Anticancer Research,* vol. 36, no. 3, pp. 1371-1378, 2016.

[23] J. W. Lee, K. Ratnakumar, K. F. Hung, D. Rokunohe, and M. Kawasumi, "Deciphering UV-induced DNA Damage Responses to Prevent and Treat Skin Cancer," (in eng), *Photochemistry and photobiology,* vol. 96, no. 3, pp. 478-499, May 2020.

[24] J. Cadet, E. Sage, and T. Douki, "Ultraviolet radiation-mediated damage to cellular DNA," *Mutation Research/Fundamental and Molecular Mechanisms of Mutagenesis,* vol. 571, no. 1, pp. 3-17, 2005/04/01/ 2005.

[25] C. A. Juan, J. M. Pérez de la Lastra, F. J. Plou, and E. Pérez-Lebeña, "The Chemistry of Reactive Oxygen Species (ROS) Revisited: Outlining Their Role in Biological Macromolecules (DNA, Lipids and Proteins) and Induced Pathologies," *International journal of molecular sciences,* vol. 22, no. 9, p. 4642, 2021.

[26] S. Emmert, M. P. Schön, and H. A. Haenssle, "Molecular Biology of Basal and Squamous Cell Carcinomas," in *Sunlight, Vitamin D and Skin Cancer*. New York, NY: Springer New York, 2014, pp. 234-252.

[27] J. B. Loureiro, M. Abrantes, P. A. Oliveira, and L. Saraiva, "P53 in skin cancer: From a master player to a privileged target for prevention and therapy," (in eng), *Biochimica et biophysica acta. Reviews on cancer,* vol. 1874, no. 2, p. 188438, Dec 2020.

[28] G. T. Bowden, "Prevention of non-melanoma skin cancer by targeting ultraviolet-B-light signalling," (in eng), *Nature reviews. Cancer,* vol. 4, no. 1, pp. 23-35, Jan 2004.

[29] M. Barthelman, W. Chen, H. L. Gensler, C. Huang, Z. Dong, and G. T. Bowden, "Inhibitory Effects of Perillyl Alcohol on UVB-induced Murine Skin Cancer and AP-1 Transactivation," *Cancer Research,* vol. 58, no. 4, pp. 711-716, 1998.

[30] T. B. El-Abaseri and L. A. Hansen, "EGFR Activation and Ultraviolet Light-Induced Skin Carcinogenesis," *Journal of Biomedicine and Biotechnology,* vol. 2007, p. 097939, 2007/04/23 2007.

[31] G. B. Maru, K. Gandhi, A. Ramchandani, and G. Kumar, "The role of inflammation in skin cancer," (in eng), *Advances in experimental medicine and biology,* vol. 816, pp. 437-69, 2014.

[32] M. Ciążyńska, I. Olejniczak-Staruch, D. Sobolewska-Sztychny, J. Narbutt, M. Skibińska, and A. Lesiak, "Ultraviolet Radiation and Chronic Inflammation—Molecules and Mechanisms Involved in Skin Carcinogenesis: A Narrative Review," *Life,* vol. 11, no. 4, p. 326, 2021.

[33] D. P. Lane, "Cancer. p53, guardian of the genome," (in eng), *Nature,* vol. 358, no. 6381, pp. 15-6, Jul 2 1992.

[34] K. A. Avery-Kiejda *et al.*, "P53 in human melanoma fails to regulate target genes associated with apoptosis and the cell cycle and may contribute to proliferation," (in eng), *BMC Cancer,* vol. 11, p. 203, May 27 2011.

[35] D. P. Lane and L. V. Crawford, "T antigen is bound to a host protein in SY40-transformed cells," *Nature,* vol. 278, no. 5701, pp. 261-263, 1979/03/01 1979.

[36] D. I. Linzer and A. J. Levine, "Characterization of a 54K dalton cellular SV40 tumor antigen present in SV40-transformed cells and uninfected embryonal carcinoma cells," (in eng), *Cell,* vol. 17, no. 1, pp. 43-52, May 1979.

[37] J. F. Millau, N. Bastien, and R. Drouin, "P53 transcriptional activities: a general overview and some thoughts," (in eng), *Mutation research,* vol. 681, no. 2-3, pp. 118-133, Mar-Jun 2009.

[38] D. Wolf, N. Harris, and V. Rotter, "Reconstitution of p53 expression in a nonproducer Ab-MuLV-transformed cell line by transfection of a functional p53 gene," (in eng), *Cell,* vol. 38, no. 1, pp. 119-26, Aug 1984.

[39] S. J. Baker *et al.*, "Chromosome 17 deletions and p53 gene mutations in colorectal carcinomas," (in eng), *Science,* vol. 244, no. 4901, pp. 217-21, Apr 14 1989.
[40] F. Murray-Zmijewski, D. P. Lane, and J. C. Bourdon, "p53/p63/p73 isoforms: an orchestra of isoforms to harmonise cell differentiation and response to stress," *Cell Death & Differentiation,* vol. 13, no. 6, pp. 962-972, 2006/06/01 2006.
[41] J. F. Millau, N. Bastien, and R. Drouin, "P53 transcriptional activities: a general overview and some thoughts," (in eng), *Mutation research,* vol. 681, no. 2-3, pp. 118-33, Mar-Jun 2009.
[42] O. Merkel *et al.*, "When the guardian sleeps: Reactivation of the p53 pathway in cancer," (in eng), *Mutation research,* vol. 773, pp. 1-13, Jul 2017.
[43] A. C. Joerger and A. R. Fersht, "The p53 Pathway: Origins, Inactivation in Cancer, and Emerging Therapeutic Approaches," (in eng), *Annual review of biochemistry,* vol. 85, pp. 375-404, Jun 2 2016.
[44] A. C. Joerger and A. R. Fersht, "Structural Biology of the Tumor Suppressor p53," *Annual review of biochemistry,* vol. 77, no. 1, pp. 557-582, 2008.
[45] R. Kamada, Y. Toguchi, T. Nomura, T. Imagawa, and K. Sakaguchi, "Tetramer formation of tumor suppressor protein p53: Structure, function, and applications," (in eng), *Biopolymers,* vol. 106, no. 4, pp. 598-612, Nov 4 2016.
[46] A. de Polo, V. Vivekanandan, J. B. Little, and Z.-M. Yuan, "MDMX under stress: the MDMX-MDM2 complex as stress signals hub," *Translational Cancer Research,* vol. 5, no. 6, pp. 725-732, 2016.
[47] J. C. Marine and A. G. Jochemsen, "MDMX (MDM4), a Promising Target for p53 Reactivation Therapy and Beyond," (in eng), *Cold Spring Harbor perspectives in medicine,* vol. 6, no. 7, Jul 1 2016.
[48] A. Lemos *et al.*, "Medicinal Chemistry Strategies to Disrupt the p53-MDM2/MDMX Interaction," (in eng), *Medicinal research reviews,* vol. 36, no. 5, pp. 789-844, Sep 2016.
[49] J. T. Zilfou and S. W. Lowe, "Tumor suppressive functions of p53," (in eng), *Cold Spring Harb Perspect Biol,* vol. 1, no. 5, p. a001883, Nov 2009.
[50] J. Chen, "The Cell-Cycle Arrest and Apoptotic Functions of p53 in Tumor Initiation and Progression," (in eng), *Cold Spring Harbor perspectives in medicine,* vol. 6, no. 3, p. a026104, Mar 1 2016.
[51] K. Harms, S. Nozell, and X. Chen, "The common and distinct target genes of the p53 family transcription factors," (in eng), *Cellular and molecular life sciences : CMLS,* vol. 61, no. 7-8, pp. 822-42, Apr 2004.
[52] K. Vermeulen, D. R. Van Bockstaele, and Z. N. Berneman, "The cell cycle: a review of regulation, deregulation and therapeutic targets in cancer," *Cell Proliferation,* vol. 36, no. 3, pp. 131-149, 2003.
[53] S. Adimoolam and J. M. Ford, "p53 and regulation of DNA damage recognition during nucleotide excision repair," (in eng), *DNA repair,* vol. 2, no. 9, pp. 947-54, Sep 18 2003.
[54] O. D. Schärer, "Nucleotide excision repair in eukaryotes," (in eng), *Cold Spring Harb Perspect Biol,* vol. 5, no. 10, p. a012609, Oct 1 2013.
[55] J. A. Marteijn, H. Lans, W. Vermeulen, and J. H. J. Hoeijmakers, "Understanding nucleotide excision repair and its roles in cancer and ageing," *Nature Reviews Molecular Cell Biology,* vol. 15, no. 7, pp. 465-481, 2014/07/01 2014.
[56] B. J. Aubrey, G. L. Kelly, A. Janic, M. J. Herold, and A. Strasser, "How does p53 induce apoptosis and how does this relate to p53-mediated tumour suppression?," (in eng), *Cell Death Differ,* vol. 25, no. 1, pp. 104-113, Jan 2018.
[57] S. Elmore, "Apoptosis: a review of programmed cell death," (in eng), *Toxicol Pathol,* vol. 35, no. 4, pp. 495-516, Jun 2007.
[58] J. B. Loureiro, M. Abrantes, P. A. Oliveira, and L. Saraiva, "P53 in skin cancer: From a master player to a privileged target for prevention and therapy," *Biochimica et*

Biophysica Acta (BBA) - Reviews on Cancer, vol. 1874, no. 2, p. 188438, 2020/12/01/ 2020.

[59] C. L. Benjamin, S. E. Ullrich, M. L. Kripke, and H. N. Ananthaswamy, "p53 tumor suppressor gene: a critical molecular target for UV induction and prevention of skin cancer," (in eng), *Photochemistry and photobiology,* vol. 84, no. 1, pp. 55-62, Jan-Feb 2008.

[60] C. G. Maki and P. M. Howley, "Ubiquitination of p53 and p21 is differentially affected by ionizing and UV radiation," *Molecular and Cellular Biology,* vol. 17, no. 1, pp. 355-363, 1997.

[61] L. Latonen, Y. Taya, and M. Laiho, "UV-radiation induces dose-dependent regulation of p53 response and modulates p53-HDM2 interaction in human fibroblasts," (in eng), *Oncogene,* vol. 20, no. 46, pp. 6784-93, Oct 11 2001.

[62] L. J. H. Bean and G. R. Stark, "Phosphorylation of serines 15 and 37 is necessary for efficient accumulation of p53 following irradiation with UV," *Oncogene,* vol. 20, no. 9, pp. 1076-1084, 2001/03/01 2001.

[63] R. P. Feehan and L. M. Shantz, "Molecular signaling cascades involved in nonmelanoma skin carcinogenesis," *Biochemical Journal,* vol. 473, no. 19, pp. 2973-2994, 2016.

[64] E. R. Kastenhuber and S. W. Lowe, "Putting p53 in Context," (in eng), *Cell,* vol. 170, no. 6, pp. 1062-1078, Sep 7 2017.

[65] P. A. Muller and K. H. Vousden, "p53 mutations in cancer," (in eng), *Nature cell biology,* vol. 15, no. 1, pp. 2-8, Jan 2013.

[66] E. M. Alexandrova, S. A. Mirza, S. Xu, R. Schulz-Heddergott, N. D. Marchenko, and U. M. Moll, "p53 loss-of-heterozygosity is a necessary prerequisite for mutant p53 stabilization and gain-of-function in vivo," *Cell Death & Disease,* vol. 8, no. 3, pp. e2661-e2661, 2017/03/01 2017.

[67] A. H. Conney, Y. P. Lu, Y. R. Lou, M. Kawasumi, and P. Nghiem, "Mechanisms of Caffeine-Induced Inhibition of UVB Carcinogenesis," (in eng), *Frontiers in oncology,* vol. 3, p. 144, 2013.

[68] S. Balasubramanian and R. L. Eckert, "Keratinocyte proliferation, differentiation, and apoptosis--differential mechanisms of regulation by curcumin, EGCG and apigenin," (in eng), *Toxicology and applied pharmacology,* vol. 224, no. 3, pp. 214-9, Nov 1 2007.

[69] F. J. Gómez-García, A. López López, Y. Guerrero-Sánchez, M. Sánchez Siles, F. Martínez Díaz, and F. Camacho Alonso, "Chemopreventive effect of pomegranate and cocoa extracts on ultraviolet radiation-induced photocarcinogenesis in SKH-1 mice," (in eng), *PLoS One,* vol. 15, no. 4, pp. e0232009-e0232009, 2020.

[70] C. A. Mintie *et al.*, "Protective Effects of Dietary Grape on UVB-Mediated Cutaneous Damages and Skin Tumorigenesis in SKH-1 Mice," (in eng), *Cancers,* vol. 12, no. 7, Jul 1 2020.

[71] K.-D. Tsai *et al.*, "Curcumin Protects against UVB-Induced Skin Cancers in SKH-1 Hairless Mouse: Analysis of Early Molecular Markers in Carcinogenesis," (in eng), *Evid Based Complement Alternat Med,* vol. 2012, pp. 593952-593952, 2012.

[72] C. M. Rigby *et al.*, "Role of p53 in silibinin-mediated inhibition of ultraviolet B radiation-induced DNA damage, inflammation and skin carcinogenesis," (in eng), *Carcinogenesis,* vol. 38, no. 1, pp. 40-50, Jan 2017.

[73] X. Tang *et al.*, "CP-31398 restores mutant p53 tumor suppressor function and inhibits UVB-induced skin carcinogenesis in mice," *The Journal of Clinical Investigation,* vol. 117, no. 12, pp. 3753-3764, 12/03/ 2007.

[74] B. A. Foster, H. A. Coffey, M. J. Morin, and F. Rastinejad, "Pharmacological rescue of mutant p53 conformation and function," (in eng), *Science,* vol. 286, no. 5449, pp. 2507-10, Dec 24 1999.

[75] S. Gomes *et al.*, "SLMP53-2 Restores Wild-Type-Like Function to Mutant p53 through Hsp70: Promising Activity in Hepatocellular Carcinoma," *Cancers,* vol. 11, no. 8, p. 1151, 2019.

[76] H. Ramos *et al.*, "A selective p53 activator and anticancer agent to improve colorectal cancer therapy," (in eng), *Cell reports,* vol. 35, no. 2, p. 108982, Apr 13 2021.

[77] A. S. Gomes *et al.*, "SLMP53-1 interacts with wild-type and mutant p53 DNA-binding domain and reactivates multiple hotspot mutations," (in eng), *Biochimica et biophysica acta. General subjects,* vol. 1864, no. 1, p. 129440, Jan 2020.

[78] J. Soares *et al.*, "Reactivation of wild-type and mutant p53 by tryptophanolderived oxazoloisoindolinone SLMP53-1, a novel anticancer small-molecule," (in eng), *Oncotarget,* vol. 7, no. 4, pp. 4326-4343, 2016.

[79] J. B. Loureiro *et al.*, "Targeting p53 for Melanoma Treatment: Counteracting Tumour Proliferation, Dissemination and Therapeutic Resistance," *Cancers,* vol. 13, no. 7, p. 1648, 2021.

[80] J. Soares *et al.*, "A tryptophanol-derived oxazolopiperidone lactam is cytotoxic against tumors via inhibition of p53 interaction with murine double minute proteins," *Pharmacological research,* vol. 95-96, pp. 42-52, 2015/05/01/ 2015.

[81] M. van Engeland, L. J. Nieland, F. C. Ramaekers, B. Schutte, and C. P. Reutelingsperger, "Annexin V-affinity assay: a review on an apoptosis detection system based on phosphatidylserine exposure," (in eng), *Cytometry,* vol. 31, no. 1, pp. 1-9, Jan 1 1998.

[82] M. Oparka *et al.*, "Quantifying ROS levels using CM-H2DCFDA and HyPer," *Methods,* vol. 109, pp. 3-11, 2016/10/15/ 2016.

[83] G. Muthusamy *et al.*, "Modified comet assays for the detection of cyclobutane pyrimidine dimers and oxidative base damages," *Journal of Radiation and Cancer Research,* Technical Report vol. 8, no. 1, pp. 82-86, January 1, 2017 2017.

[84] A. R. Collins, "The comet assay for DNA damage and repair," *Molecular Biotechnology,* vol. 26, no. 3, p. 249, 2004/03/01 2004.

[85] L. J. Mah, A. El-Osta, and T. C. Karagiannis, "γH2AX: a sensitive molecular marker of DNA damage and repair," *Leukemia,* vol. 24, no. 4, pp. 679-686, 2010/04/01 2010.

[86] V. Rapić-Otrin, M. P. McLenigan, D. C. Bisi, M. Gonzalez, and A. S. Levine, "Sequential binding of UV DNA damage binding factor and degradation of the p48 subunit as early events after UV irradiation," (in eng), *Nucleic acids research,* vol. 30, no. 11, pp. 2588-98, Jun 1 2002.

[87] Q.-E. Wang *et al.*, "Ubiquitylation-independent degradation of Xeroderma pigmentosum group C protein is required for efficient nucleotide excision repair," *Nucleic acids research,* vol. 35, no. 16, pp. 5338-5350, 2007.

[88] K. Kyrylkova, S. Kyryachenko, M. Leid, and C. Kioussi, "Detection of Apoptosis by TUNEL Assay," in *Odontogenesis: Methods and Protocols*, C. Kioussi, Ed. Totowa, NJ: Humana Press, 2012, pp. 41-47.

[89] E. Martynova *et al.*, "Gain-of-function p53 mutants have widespread genomic locations partially overlapping with p63," (in eng), *Oncotarget,* vol. 3, no. 2, pp. 132-143, 2012.

[90] N. Bissonnette and D. J. Hunting, "p21-induced cycle arrest in G1 protects cells from apoptosis induced by UV-irradiation or RNA polymerase II blockage," *Oncogene,* vol. 16, no. 26, pp. 3461-3469, 1998/07/01 1998.

[91] A. H. Boulares *et al.*, "Role of Poly(ADP-ribose) Polymerase (PARP) Cleavage in Apoptosis: CASPASE 3-RESISTANT PARP MUTANT INCREASES RATES OF APOPTOSIS IN TRANSFECTED CELLS *," *Journal of Biological Chemistry,* vol. 274, no. 33, pp. 22932-22940, 1999.

[92] S. Wu, H. N. Loke, and A. Rehemtulla, "Ultraviolet radiation-induced apoptosis is mediated by Daxx," (in eng), *Neoplasia,* vol. 4, no. 6, pp. 486-492, Nov-Dec 2002.

[93] D. Liu and Y. Xu, "p53, oxidative stress, and aging," (in eng), *Antioxid Redox Signal,* vol. 15, no. 6, pp. 1669-1678, 2011.

[94] M. J. Morgan, Y.-S. Kim, and Z.-g. Liu, "TNFα and reactive oxygen species in necrotic cell death," *Cell Research,* vol. 18, no. 3, pp. 343-349, 2008/03/01 2008.

[95] J. Shao *et al.*, "Overexpression of the wild-type p53 gene inhibits NF-kappaB activity and synergizes with aspirin to induce apoptosis in human colon cancer cells," (in eng), *Oncogene,* vol. 19, no. 6, pp. 726-36, Feb 10 2000.

[96] S. Pillai, C. Oresajo, and J. Hayward, "Ultraviolet radiation and skin aging: roles of reactive oxygen species, inflammation and protease activation, and strategies for prevention of inflammation-induced matrix degradation - a review," (in eng), *International journal of cosmetic science,* vol. 27, no. 1, pp. 17-34, Feb 2005.

[97] M. S. Matsui, N. Wang, and V. A. DeLeo, "Ultraviolet radiation B induces differentiation and protein kinase C in normal human epidermal keratinocytes," *Photodermatology, Photoimmunology & Photomedicine,* vol. 12, no. 3, pp. 103-108, 1996.

[98] K. Krishnan, S. Campbell, F. Abdel-Rahman, S. Whaley, and W. L. Stone, "Cancer chemoprevention drug targets," (in eng), *Current drug targets,* vol. 4, no. 1, pp. 45-54, Jan 2003.

[99] A. M. Bode and Z. Dong, "Targeting signal transduction pathways by chemopreventive agents," (in eng), *Mutation research,* vol. 555, no. 1-2, pp. 33-51, Nov 2 2004.

Annexes

Oral Communications

1. **SIFFUP November 24th 2020: Simpósio de Investigação da Faculdade de Farmácia da Universidade do Porto**

SLMP53-2: A MUTANT P53 REACTIVATOR WITH PROMISING ACTIVITY IN SKIN CANCER PREVENTION

Rita Ribeiro[1]*, Joana B. Loureiro[1], Nair Nazareth[1], Tiago Ferreira[3], Valentina Barcherini[2], Paula A. Oliveira[3], Maria M. M. Santos[2], Lucília Saraiva[1]
*Presenting author

[1]LAQV/REQUIMTE, Laboratório de Microbiologia, Departamento de Ciências Biológicas, Faculdade de Farmácia, Universidade do Porto, Porto, Portugal; [2]iMed.ULisboa, Faculdade de Farmácia, Universidade de Lisboa, Lisboa, Portugal; [3]CITAB, Departamento de Ciências Veterinárias, Escola de Ciências Veterinárias e Agrárias, Universidade de Trás os Montes e Alto Douro, Vila Real, Portugal.

Skin cancer (SC) is among the most incident type of cancer within the white population. Ultraviolet radiation (UVR) is the major environmental risk factor associated with SC [1]. Its major effects on skin include DNA damage, particularly cyclobutane pyrimidine dimers (CPD) and 6-4 pyrimidone photoprodutcs (6-4PP) formation, inflammation, and reactive oxygen species (ROS) production. p53 is a tumor suppressor with a crucial role in DNA damage repair, particularly in the nucleotide excision repair (NER) pathway induction. Mutant p53 (mutp53), namely mutations with UVR signatures, are present in early events of carcinogenesis [2]. The increasing rates of SC over the years have suggested that the current preventive approaches, such as the use of sunscreen, have been not enough to counteract this health concern [3]. Therefore, it has been essential to pursue for new pharmacological opportunities towards SC prevention. The reactivation of wild-type-like function to mutp53 by small molecules represents a promising strategy of UVR-induced SC prevention. Recently, our group identified the tryptophanol-derived oxazoloisoindolinone SLMP53-2 as a new mutp53-reactivating agent [4,5]. With this work, we aimed to study the potential of SLMP53-2 as chemopreventive agent against SC formation. Pre-treatment of

human normal keratinocytes with SLMP53-2, at a concentration with no significant effect on cell proliferation, 24h before UVB irradiation, increased cell survival and reduced DNA damage, with regulation of major proteins of the NER pathway, ROS production, and the expression levels of inflammatory markers. Consistently, *in vivo* analysis, showed a decrease in the percentage of CPD positive cells in SLMP53-2-pre-treated mice irradiated with UVB. Altogether, these results indicate that SLMP53-2 has promising protective activity against skin carcinogenesis. Further *in vivo* studies are underway to validate the potential application of SLMP53-2 in SC prevention.

[1] Apalla Z, et al. Dermatol Pract Concept. 2017 Apr 30;7(2):1-6 [2] Loureiro, J. B., et al. Biochimica et Biophysica Acta (BBA) - Reviews on Cancer. 2020, 1874(2), 188438. [3] Benjamin CL et al. Photochem Photobiol. 2008;84(1):55–62; [4] European patent n° EP14739561.0/ US patent n° 20160347765, 2016; [5] Gomes S et al. Cancers. 2019 11(8), 1151.

This work received financial support from PT national funds (FCT/MCTES, Fundação para a Ciência e Tecnologia and Ministério da Ciência, Tecnologia e Ensino Superior) through grant UID/QUI/50006/2020. FCT fellowships: SFRH/BD/128673/2017 (J. B. Loureiro) and from Liga Portuguesa contra o Cancro - Núcleo Regional do Norte (FCT / MCTES, Fundação para a Ciência e Tecnologia e Ministério da Ciência, Tecnologia e Ensino Superior) through grant UIDB / 50006/2020.

This work was awarded 1st prize at SIFFUP 14th edition.

2. IJUP 14th Edition May 5th 2021 – Encontro de Investigação Jovem da Universidade do Porto

CHEMOPREVENTION OF SKIN CANCER THROUGH THE MUTANT P53 REACTIVATOR SLMP53-2

Rita Ribeiro[1]*, Joana B. Loureiro[1], Nair Nazareth[1], Tiago Ferreira[3], Valentina Barcherini[2], Paula A. Oliveira[3], Maria M. M. Santos[2], Lucília Saraiva[1]

[1]LAQV/REQUIMTE, Laboratório de Microbiologia, Departamento de Ciências Biológicas, Faculdade de Farmácia, Universidade do Porto, Porto, Portugal; [2]iMed.ULisboa, Faculdade de Farmácia, Universidade de Lisboa, Lisboa, Portugal; [3]CITAB, Departamento de Ciências Veterinárias, Escola de Ciências Veterinárias e Agrárias, Universidade de Trás os Montes e Alto Douro, Vila Real, Portugal.

*Presenting author.

Ultraviolet radiation (UVR) is the major environmental risk factor associated with skin cancer (SC), which incidence has been increasing globally [1]. One of the main biological effects of UVR on skin is the induction of DNA damages, potentially causing protein mutations [1]. Mutant p53 (mutp53), namely mutations with UVR signature, are generated in early phases of skin carcinogenesis, having crucial role in tumor development [1]. The rising rates of SC incidence worldwide demonstrate that the current preventive approaches, such as the use of sunscreen, have not been effective [1]. Hence, the development of novel pharmacological opportunities towards SC prevention is crucial to counteract its incidence. The reactivation of mutp53 by small molecules represents a promising strategy for UVR-induced SC prevention. Recently, our group identified a new mutp53-reactivating agent, the tryptophanol-derived oxazoloisoindolinone SLMP53-2. In this work, we aimed to evaluate the potential SLMP53-2 as chemopreventive agent against UVB-induced SC formation. Pre-treatment of human normal keratinocytes with SLMP53-2, 24h before UVB irradiation, increased cell survival and reduced DNA damage, with up-regulation of major proteins of the NER pathway and down-regulation of inflammatory markers. Importantly, *in vivo* analysis, also showed a decrease in the percentage UVB-induced DNA damages in SLMP53-2-pre-treated mice irradiated with UVB. Overall, the obtained results indicate a potential preventive activity for SLMP53-2 against skin carcinogenesis.

Additional *in vivo* studies are underway to validate SLMP53-2 as chemopreventive agent.

[1] Loureiro, J. B., et al. Biochim Biophys Acta Rev Cancer 2020, 1874(2), 188438.; [2] Gomes, S., et al. Cancers 2019, 11(8), 1151.

Acknowledgements: FCT/MCTES - projects UIDB/50006/2020, UIDP/04423/2020; FCT fellowships: SFRH/BD/128673/2017 (J. B. Loureiro); Liga Portuguesa contra o Cancro – N.R.N. (FCT / MCTES) - grant UIDB/50006/2020.

This work was awarded best oral communication distinction on the Health Sciences panel at IJUP 14th edition.